J. Mol. Model. **1997**, *3*, 78 – 116

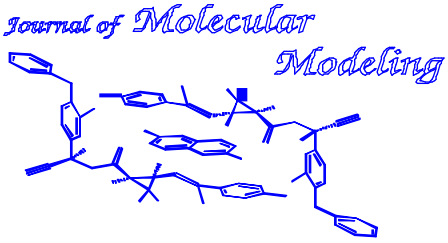

Davydov Soliton Dynamics in Proteins: III. Applications and Calculation of Vibrational Spectra

Wolfgang Förner

Chair for Theoretical Chemistry and Laboratory of the National Foundation of Cancer Research at the Friedrich-Alexander University Erlangen-Nümberg, Egerlandstr. 3, D-91058 Erlangen, FRG. (foerner@pctc.chemie.uni-erlangen.de)

Present address: Chemistry Department, King Fahd University of Petroleum and Minerals, Dhahran 31261, Saudi Arabia

Received: 5 July 1996 / Accepted: 27 January 1997 / Published: 7 February 1997

Abstract

The mechanism for energy and signal transport in proteins as suggested by Davydov is discussed. The idea is based on a coupling of amide-I oscillators to acoustic phonons in a hydrogen bonded chain. Results as obtained with the usually used ansätze are discussed. The quality of these states for an approximate solution of the time-dependent Schrödinger equation is investigated. It is found that the semiclassical ansatz is a poor approximation, while the more sophisticated $|D_1>$ state seems to represent the exact dynamics quite well. This was shown by extensive calculations, both analytically and numerically in the two preceding papers. Calculations at a temperature of 300K for one chain, as well as for three coupled ones (as they are present in an α-helix) are presented and discussed. From the calculations it is evident, that Davydov solitons are stable for reasonable parameter values at 300K for special initial excitations close to the terminal sites of the chain. Further vibrational spectra are presented and discussed. Our results suggest, that due to their strong dependence on the initial state, the Davydov $|D_1>$ model system might be a (quantum) chaotic one.

Keywords: Proteins, Davydov model, dynamics, vibrational spectra

Introduction

A recent review of Davydov soliton theory and its implications was given by Scott [1]. A basic problem in biophysics is the storage and transport of energy through protein chains. This energy in biological systems is released by the hydrolysis of adenosinetriphosphate (ATP) molecules which amounts to about 0.4 eV (see [1–5] for further details and references). It was Davydov's [2–5] idea that the best candidate for storing this energy in proteins is the amide-I vibration, which is essentially of C=O stretch type, because one quantum of this vibration has an energy of 0.205 eV, roughly half of the energy released by ATP hydrolysis. From this starting point Davydov developed his physical model for the energy transport. In α–helical proteins the C=O groups of a turn in the helix form hydrogen bonds to the N-H groups in the next turn. As indicated in the following sketch (see section II) these hydrogen bonds are coupled harmonically to each other in chains parallel to the helix axis and perpendicular to the covalent backbone. There are always three parallel chains of this kind in an α–helix. Within such a chain the C=O oscilla-

tors are coupled via their transition dipole moment with each other. This type of coupling is a linear one and makes the system dispersive. However, the chain of linearly coupled hydrogen bonds forms a phonon system. Since the excitation energy of the amide-I oscillators is naturally dependent on the length of the hydrogen bond in which the C=O group takes part, the system of amide-I oscillators is coupled to the acoustic phonon system of the hydrogen bonded chain (the so-called lattice). This makes the system non-linear and thus it could be possible that an initially localized excitation would not disperse, but travel in the chain as a solitary wave. The coupling constant can be estimated experimentally. These experimental estimates place its value in a region between 20 and 70 pN.

These basic concepts of the Davydov soliton mechanism for energy transport in proteins [2-5], as well as the different attempts to include the effects of finite temperature into the model [4-13] and the controversy about thermal stability of protein solitons is discussed in [1,6] and in our previous papers [14, 15]. Therefore we do not want to elaborate on these points here. The extensive discussion on the validity of the different ansatz states used in the literature [16-25] is also reviewed there [6, 14, 15]. Numerous possibilities for applications of these ideas also to other systems are discussed again by Scott in his review [1]. One should mention, that for a simplified semiclassical $|D_2\rangle$ ansatz it was found that the stability of solitons increases with the number of amide-I quanta they carry (see e.g. [1, 8c]). However, to the knowledge of the author, it was never investigated whether or not this is also true for the so-called $|D_1\rangle$ ansatz, which includes quantum effects in the lattice, where the equations of motion for multi-quanta states are far more complex than in the $|D_2\rangle$ case [24], where just the norm of the state has to be changed to q in case of q quanta. In the equations of motion for the $|D_1\rangle$ state the norm simply cancels. In a series of papers we dealt mainly with ansatz states which include quantum effects in the lattice into the description and with the inclusion of effects of finite temperature into these theories [6, 14, 15, 22, 27-30]. However, since the $|D_2\rangle$ state is often used in the literature and exact solutions for it are available, we discuss this state and the results of its numerical applications also in the present work. Furthermore, the use of adiabatic ansätze in the spirit of $|D_2\rangle$ in other systems might be justified and thus the investigations of the properties of this ansatz is of interest by itself.

Since we are extending at present the application of $|D_1\rangle$ type ansatz states also to the case of polyacetylene [31] and other conducting polymers, it was desirable to obtain detailed informations on the limitations of this ansatz. For this purpose we had expanded the exact solution $|\Phi\rangle = \exp\left[-i\hat{H}_D t/\hbar\right]|\Phi_0\rangle$ for the Davydov Hamiltonian ($\hat{H}_D$), where $|\Phi_0\rangle$ is the initial state, in a Taylor series in time and compared the results with those from a $|D_1\rangle$ simulation in the previous papers of this series [14, 15]. In this way we found a good agreement between the short time dynamics obtained in this way and by a $|D_1\rangle$ simulation [14, 15] (parts of this work can be found also in [32]). Attempts into this direction have been reported also previously by Cruzeiro-Hansson, Christiansen and Scott [33]. After discussing the validity of ansatz states in [14, 15], we want to give in this work a variety of applications of these ansätze to proteins. For this purpose, we do not want to discuss only the more correct $|D_1\rangle$ state, but also the results obtained from its semiclassical, adiabatic counterpart, the so-called $|D_2\rangle$ state. We decided to present also these results and a short discussion of the validity of this state because, as mentioned above, it is still widely used in the literature, also in applications to other systems.

However, mainly we are concerned with the $|D_1\rangle$ state. Since it was found previously [14, 15] that this ansatz provides a reasonably exact description of the dynamics of initial excitations in the Davydov model, we apply it in this work also to compute spectra and review some recent experimental results in view of our theoretical spectra. Further we discuss in some detail why it would be more or less impossible to detect Davydov solitons by conventional vibrational spectroscopy. From this we conclude, that spectroscopic experiments which failed [39] to detect Davydov solitons in proteins cannot be viewed as a prove for the non-existence of them. Reviews on recent experimental and theoretical results on biomolecules including proteins and DNA can be found in [39], where also recent considerations on solitons and bisolitons in DNA and proteins are discussed.

The Davydov Model for α-Helical Proteins

In order to make this paper self-contained we want to repeat here briefly the basic properties of the Davydov model, although they can be found in [14]. However, the discussion in the previous papers of this series are quite extensive, and we will refer in this work to the derivations and results presented there in several cases. The Hamiltonian introduced by Davydov for proteins has been discussed extensively in the literature. However, for the purpose of clearcut definitions in the following, we repeat the basic formulas here. The Davydov Hamiltonian for our problem [2] in its spatial representation reads as

$$\hat{H}_D = \sum_n \Big[E_0 \hat{a}_n^+ \hat{a}_n - J\left(\hat{a}_n^+ \hat{a}_{n+1} + \hat{a}_{n+1}^+ \hat{a}_n\right) + \frac{\hat{p}_n^2}{2M} + \frac{W}{2}(\hat{q}_{n+1} - \hat{q}_n)^2 + \chi \hat{a}_n^+ \hat{a}_n \left(\hat{q}_{n+1} - \hat{q}_n\right) \Big] \qquad (1)$$

In eq. (1) $\hat{a}_n^+ (\hat{a}_n)$ are the usual boson creation (annihilation) operators for the amide-I oscillators at sites n (see following sketch), while the displacement ($\hat{q}_n$) and momentum ($\hat{p}_n$) operators refer to the amino acid residues at site n.

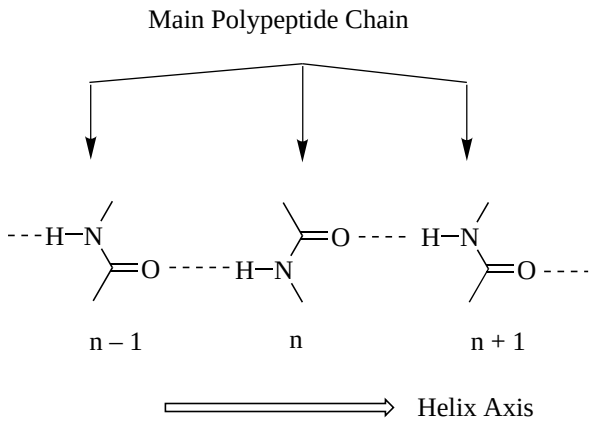

The amino acid residues are bound covalently to the protein backbone, which has a helical structure and our units n-1, n, n+1 are situated in neighboring turns of this helix. Within the backbone the residue no. n+1 is just the fourth one from the residue no. n. From infrared spectra the excitation energy of an isolated amide-I oscillator can be deduced (E_0=0.205 eV). Usually for all parameters in eq. (1) site-independent mean values are used. The average value for the coupling of the transition dipole moments of neighboring amide-I oscillators (only first neighbor interactions are explicitely taken into account) is J=0.967 meV. The average spring constant of the hydrogen bonds is taken usually to be W=13 N/m, as measured in crystalline formamide. $\hat{p}_n$ is the momentum and $\hat{q}_n$ the position operator of unit n. The mass M of a peptide unit is taken as the mean value of the masses of the units in myosine (M=114m_p; m_p is the proton mass). The energy of the CO stretching vibration in hydrogen bonds is a function of the length r of the hydrogen bond ($E=E_0+\chi r$). For χ the experimental estimates are 35 pN and 62 pN. Ab initio calculations on formamide dimers usually lead to χ = 30–50 pN. However, with small basis set *ab initio* Hartree-Fock calculations (no electron-electron correlations included), wrong results, even negative values for χ were obtained (see e.g. [1] for a review and references). Note, that in the model a given amide-I oscillator interacts only with that hydrogen bond of the chain, in which the CO bond is directly involved, since interactions with other hydrogen bonds are much smaller, and thus negligible.

The one-particle Hamiltonian [2, 3], where one-particle refers to the quanta of the amide-I vibration, in second quantized form is given by

$$\hat{H}_D = \sum_{n=1}^{N}\left[E_0\,\hat{a}_n^+\hat{a}_n - J\left(\hat{a}_{n+1}^+\hat{a}_n + \hat{a}_n^+\hat{a}_{n+1}\right)\right] + \\ + \sum_{k=1}^{N-1}\hbar\omega_k\left[\hat{b}_k^+\hat{b}_k + \frac{1}{2} + \sum_{n=1}^{N}B_{nk}\left(\hat{b}_k + \hat{b}_k^+\right)\hat{a}_n^+\hat{a}_n\right] \qquad (2)$$

$$B_{nk} = \frac{\chi}{\omega_k}\frac{1}{\sqrt{2M\hbar\omega_k}}[U_{n+1,k} - U_{nk}]\,; \quad \omega_N = 0\,; \quad k \neq N$$

Note, that a remark of Kapor [34] concerning the role of the lattice in a special case (decoupled) does not apply as shown in [14]. $\hat{b}_k^+\left(\hat{b}_k\right)$ are creation (annihilation) operators for acoustic phonons of wave number k. The translational mode has to be excluded from all summations. In the simulations presented we use the asymmetric interaction model where, as mentioned above, only the coupling of the oscillator n to the hydrogen bond between n and n+1, in which the oscillator takes part, is considered. ω_k denotes the eigenfrequency of the normal mode k and $\underline{\underline{U}}$ contains the normal mode coefficients. $\underline{\omega}$ and $\underline{\underline{U}}$ are obtained by diagonalization of the matrix $\underline{\underline{V}}$ with elements

$$V_{nm} = \frac{W}{M}\left\{\left(2-\delta_{n1}-\delta_{nN}\right)\delta_{nm} - \left(1-\delta_{nN}\right)\delta_{m,n+1} - \right. \\ \left. - \left(1-\delta_{n1}\right)\delta_{m,n-1}\right\} \qquad (3)$$

$$\left(\underline{\underline{U}}^+\,\underline{\underline{\underline{V}}}\,\underline{\underline{U}}\right)_{kk'} = \omega_k^2\delta_{kk'} \qquad ; \qquad \underline{\underline{U}}^+\,\underline{\underline{U}} = \underline{\underline{U}}\,\underline{\underline{U}}^+ = \underline{\underline{1}}$$

This form of $\underline{\underline{V}}$ implies that we use an open chain and N units (see [37]). Thus the terminal units of our chain are as shown in the following sketch, indicating that the left terminus of the chain contains a free NH bond, while the right terminus has a free CO bond. Both of them, however, could be connected to random-coil, β-pleated sheet or enzymatically active regions of different structure (e.g. catalysing ATP hydrolysis).

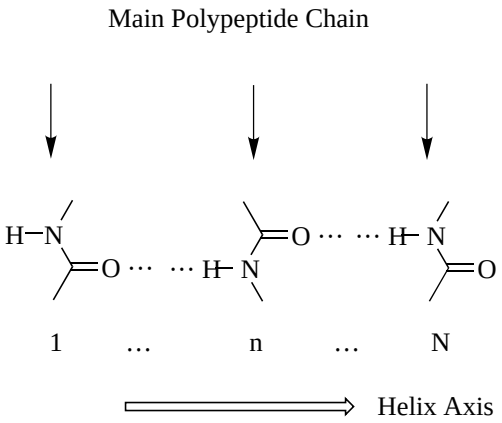

General Treatment of Time-Dependent Ansatz States

To solve the time dependent Schrödinger equation (approximately)

$$i\hbar\frac{\partial}{\partial t}|\psi> \;=\; \hat{H}|\psi> \tag{4}$$

we can always introduce an appropriate ansatz with a set of time dependent unknown parameters $\underline{x}(t)$

$$|\psi> \;=\; |\psi[\underline{x}(t)]> \tag{5}$$

For the optimization of these parameters as function of time we have several options. In this work we prefer the Lagrangian method, following Skrinjar et al. [19]. Then first of all we have to evaluate the Lagrangian of our system:

$$L\left[\underline{x}(t),t\right] = \frac{i\hbar}{2}\left(<\psi|\frac{\partial}{\partial t}\psi> - <\frac{\partial}{\partial t}\psi|\psi>\right) - <\psi|\hat{H}|\psi> \tag{6}$$

With the usual variatonal treatment (in our case the norm is automatically conserved and thus no additional Lagrange multiplier is necessary)

$$\delta\int_{t_1}^{t_2} L\left[\underline{x}(t),t\right]dt \;=\; 0 \tag{7}$$

we obtain finally the equations of motion for our parameters from the Euler-Lagrange equations

$$\frac{d}{dt}\frac{\partial L\left[\underline{x}(t),t\right]}{\partial\dot{\underline{x}}(t)} - \frac{\partial L\left[\underline{x}(t),t\right]}{\partial\underline{x}(t)} \;=\; 0 \tag{8}$$

It can easily be shown by a sequence of partial integrations in eq. (9), that this method is completely equivalent to the application of Frenkel's time-dependent variational principle [31]:

$$\delta\int_{t_1}^{t_2} <\psi|\left(i\hbar\frac{\partial}{\partial t} - \hat{H}\right)|\psi>\, dt \;=\; 0 \tag{9}$$

Again completely equivalent would be the use of Heisenberg equations for time-dependent operators [19] or of Hamilton's principle in the form (H is the expectation value of the Hamiltonian) [19]

$$\delta\int_{t_1}^{t_2}\left(H\left[\underline{x}(t),t\right] - \left(\frac{\partial L\left[\underline{x}(t),t\right]}{\partial\dot{\underline{x}}}\right)^{tr}\cdot\dot{\underline{x}}\right)dt \;=\; 0 \tag{10}$$

where superscript tr denotes the transpose of the vector. In case of the $|D_1>$ state (see below), Davydov [2,3] used a form of Hamilton's method, which leads to incorrect equations (later applied by numerous authors), because, as Skrinjar et al. [19] point out, in that case the choice of canonically conjugated variables is quite ambiguous (the Lagrangian is linear in the generalized velocities).

The Semiclassical $|D_2>$ Ansatz

The most simple form of an ansatz for $|\psi>$ is the so-called $|D_2>$ state, suggested first by Davydov [2], which is a product state of the exact solutions for the isolated oscillators and the isolated amide-I subsystem with unknown time-dependent parameters:

$$|D_2> \;=\; \sum_n a_n(t)\hat{a}_n^+|0>_e\,\hat{U}|0>_p \tag{11}$$

where

$$\hat{U}|0>_p \;=\; \exp\left[-\frac{1}{2}\left|\sum_k b_k(t)\right|^2\right]\cdot\exp\left[\sum_k b_k(t)\,b_k^+\right]|0>_p$$
$$\;=\; \exp\left\{\sum_k\left[b_k(t)\,\hat{b}_k^+ - b_k^*(t)\,\hat{b}_k\right]\right\}|0>_p \tag{12}$$

The $b_k(t)$ are the coherent state amplitudes and $|a_n(t)|^2$ is the probability to find an amide-I quantum at site n. These are the quantities which have to be determined. Note, that the second form of the lattice part holds only if the operator acts on the phonon vacuum $|0>_p$ ($|0>_e$ is the exciton vacuum for the amide-I vibrations). The second variant of the lattice part of the state can be written also in the form

$$\hat{U}|0>_p = \exp\left\{\frac{i}{\hbar}\sum\left[\left\langle\hat{q}_m(t)\right\rangle\hat{p}_m - \left\langle\hat{p}_m(t)\right\rangle\hat{q}_m\right]\right\}|0>_p \tag{13}$$

where now the expectation values of the displacement and momentum operators are the unknown quantities. Physically, this ansatz assumes, that the amide-I oscillators would not excite lattice phonons according to their individual excitation states, but in an averaged way.

Equations of Motion

The equations of motion for the $|D_2>$ state containing one quantum of amide-I vibration can be derived by the Lagrangian method described above and subsequently be transformed from the normal mode to the coordinate representation:

$$\begin{aligned} i\hbar\,\dot{a}_n &= -J\left(a_{n+1}+a_{n-1}\right)+\chi\left(q_{n+1}-q_n\right)a_n \\ \dot{p}_n &= W\left(q_{n+1}-2q_n+q_{n-1}\right)+\chi\left(|a_n|^2-|a_{n-1}|^2\right) \\ \dot{q}_n &= \frac{p_n}{M} \end{aligned} \tag{14}$$

The numerical solution of these equations can be accomplished with the help of a fourth order Runge-Kutta method. However, in the continuum approximation the equations can be solved also analytically. But our results indicate, that the widths of solitons in the discrete case are too small to justify that approximation [13b]. Note, that the lattice parts of eq. (15) are not entirely classical as their form might suggest, but the q_n's and p_n's have to be viewed as expectation values of the corresponding quantum mechanical operators rather than as classical variables. However, the $|D_2>$ state is the exact solution for $\hat{H}_D$ if the operators of the displacements and momenta are replaced by real numbers $q_n(t)$ and $p_n(t)$, respectively [35, 36]. In the case of Q quanta of amide-I vibration which all occupy the same state, only the equations of motion for the time derivative of the lattice momenta [eq. (15)] change to [8]

Applications

The numerical results show, that for one-quantum states solitons at T = 0 K can be formed, and appear in the region of χ larger than roughly 40 pN for a spring constant of 13 N/m for the hydrogen bonds. Further it turns out [1,8] that the stability of the solitons increases, when the number of amide-I quanta they carry is increased. In Figure1 we show our simulations for a two-quanta state for three different values of χ. The plots show for each simulation the probability $|a_n|^2$ to find the two amide-I quanta at site n and at time t, and in addition the square of the local lattice deformation $D_n = (q_{n+1}-q_n)^2$ again as function of site n and time t. It is obvious, that at a coupling χ = 20 pN the excitation disperses, and in the lattice we see only the shock wave coming from the initial excitation and travelling with the speed of sound through the chain. If we increase the coupling to 30 pN clearly a solitary wave is formed, which travels without dispersion through the chain and survives the reflection at the chain end. In this case we recognize in the plot of the squared lattice deformation, which is proportional to the local potential energy of the lattice, that in addition to the shock wave a deformation follows the soliton, and stabilizes it against dispersion. Clearly, for a larger coupling, the speed of the excitation wave becomes smaller. This is evident for the case of χ = 40 pN and at χ = 62 pN (not shown here) the soliton becomes pinned at the initial excitation site. Note, that the width of the soliton is far too small to justify a continuum approximation.

In Figure 2 we show the interesting case of two solitary waves which collide in the center of the chain. These simulations are performed again with two quanta of amide-I oscillation, however, each quantum is localized initially at the two different terminal sites of the chain. Thus from each chain end a one-quantum wave starts to travel through the chain and solitons form only for couplings larger than roughly 40 pN in contrast to the previous case where both quanta were located within one wave. For coupling constants between 40 pN and roughly 60 pN the two solitary waves collide and penetrate each other without a visible interaction between them (Figure 2a). However from χ = 62 pN (Figure 2b) a new phenomenon occurs, namely one of the two solitons takes a fraction of the amide-I quantum contained in the other one, which after the interaction disperses, while the former one travels with a larger amplitude and reduced velocity to the chain end where it is reflected. The asymmetry of the two solitary waves originates in the above discussed asymmetry of the two terminal amino acid residues of a chain. Starting from roughly 70 pN coupling strength, the two one-quantum solitons repell each other i.e. their velocity becomes smaller, the closer they get and after the collision they fuse to a single, pinned two-quantum soliton (Figure 2c).

Thus, we can conclude that solitons exist in the Davydov model for reasonable values of the parameters at T = 0 K, if the $|D_2>$ ansatz would be a reliable approximation. This problem is dealt with below. First we want to concentrate on temperature effects.

Temperature Effects

Basically for the semi-classical $|D_2>$ ansatz there are two models for the inclusion of temperature effects into the theory. First of all we can populate the normal modes of the lattice prior to the initial amide-I excitation with a thermal distribution of phonons according to Bose-Einstein statistics [12,13]. The other, widely used method is the application of a Langevin equation to the lattice. This reads as

$$\begin{aligned} M\,\ddot{q}_n &= W\left(q_{n+1}-2q_n+q_{n-1}\right)+ \\ &\quad +\chi\left(|a_n|^2-|a_{n-1}|^2\right)+F_n(t)-M\,\Gamma\,\dot{q}_n \end{aligned} \tag{16}$$

while the equation for the oscillators remains unchanged [8]. The two additional terms correspond to degrees of freedom of the system which are not explicitely treated, i.e. they are considered as a heat bath. $F_n(t)$ are random forces with a Gaussian distribution. Via their correlation function temperature can be introduced by virtue of the fluctuation-dissipation theorem:

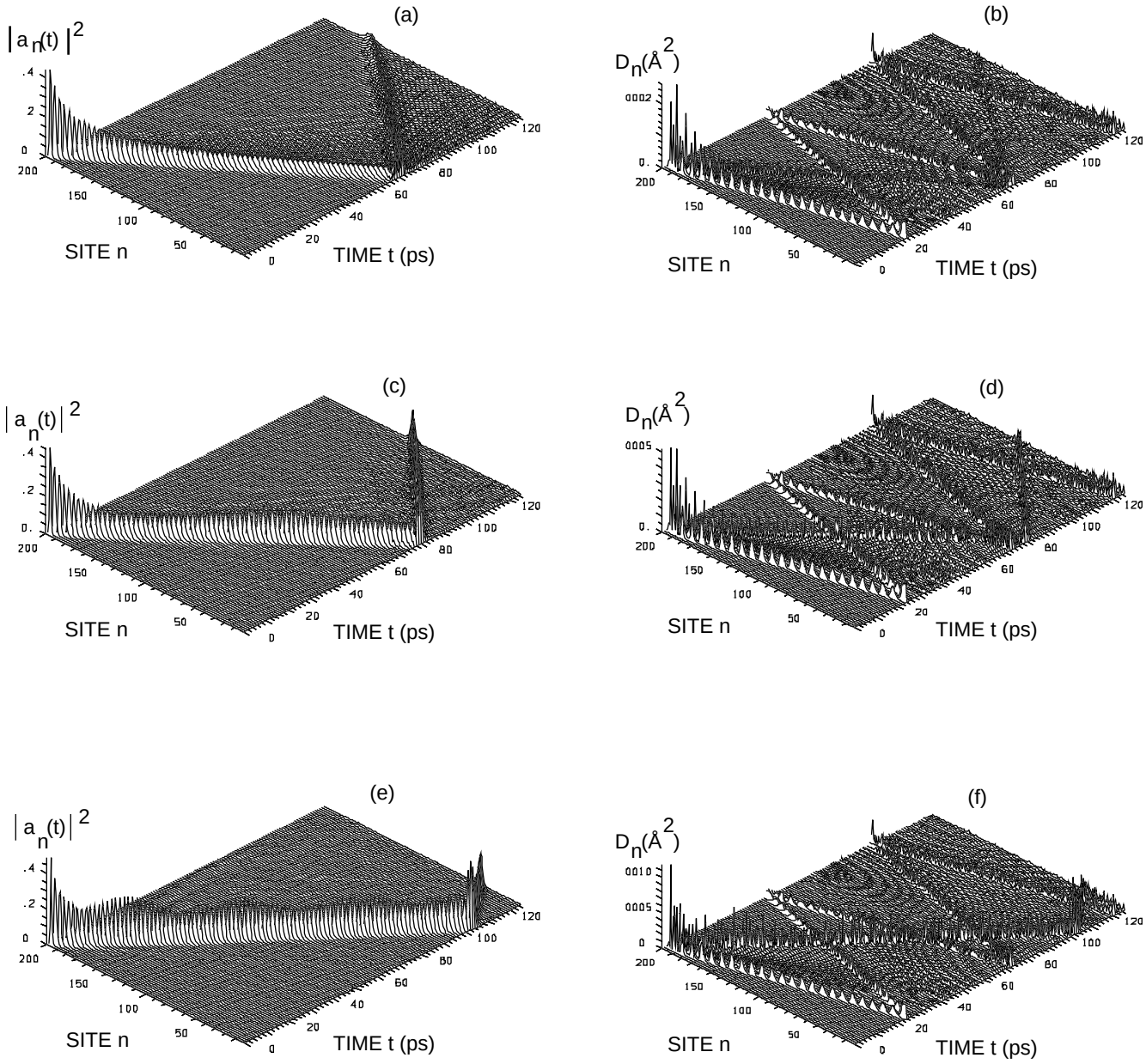

Figure 1. *The probability $|a_n|^2$ (a,c,e) and the squared local lattice deformation D_n (b,d,f) as functions of site n and time t for the time evolution of two amide-I quanta, initially localized close to the chain end (n_o=199) for J = 0.967 meV, W=13 N/m for three values of the coupling constant χ at T=0K for an open chain of 200 units, with units 1 and 200 kept fixed during the simulations in the $|D_2>$ model (the time step size was 5 fs and a 4th order Runge-Kutta method was used).*

(a,b) χ = 20 pN (c,d) χ = 30 pN (e,f) χ = 40 pN

$$< F(x,t)F(0,0) > \; = \; 2M k_B T \Gamma a \delta(x)\delta(t) \qquad (17)$$

where a is the lattice constant. Then the distribution of the random forces is

$$P(F_n) \; = \; \frac{1}{\sqrt{2\pi\sigma}} e^{-\frac{F_n^2}{2\sigma}} \; ; \; \sigma = 2M k_B T \frac{\Gamma}{\tau} \qquad (18)$$

where τ is the time step in the simulation. The random forces on one hand describe the energy, the lattice obtains from interactions with the heat bath. The friction term on the other hand describes the energy, the lattice transfers to the

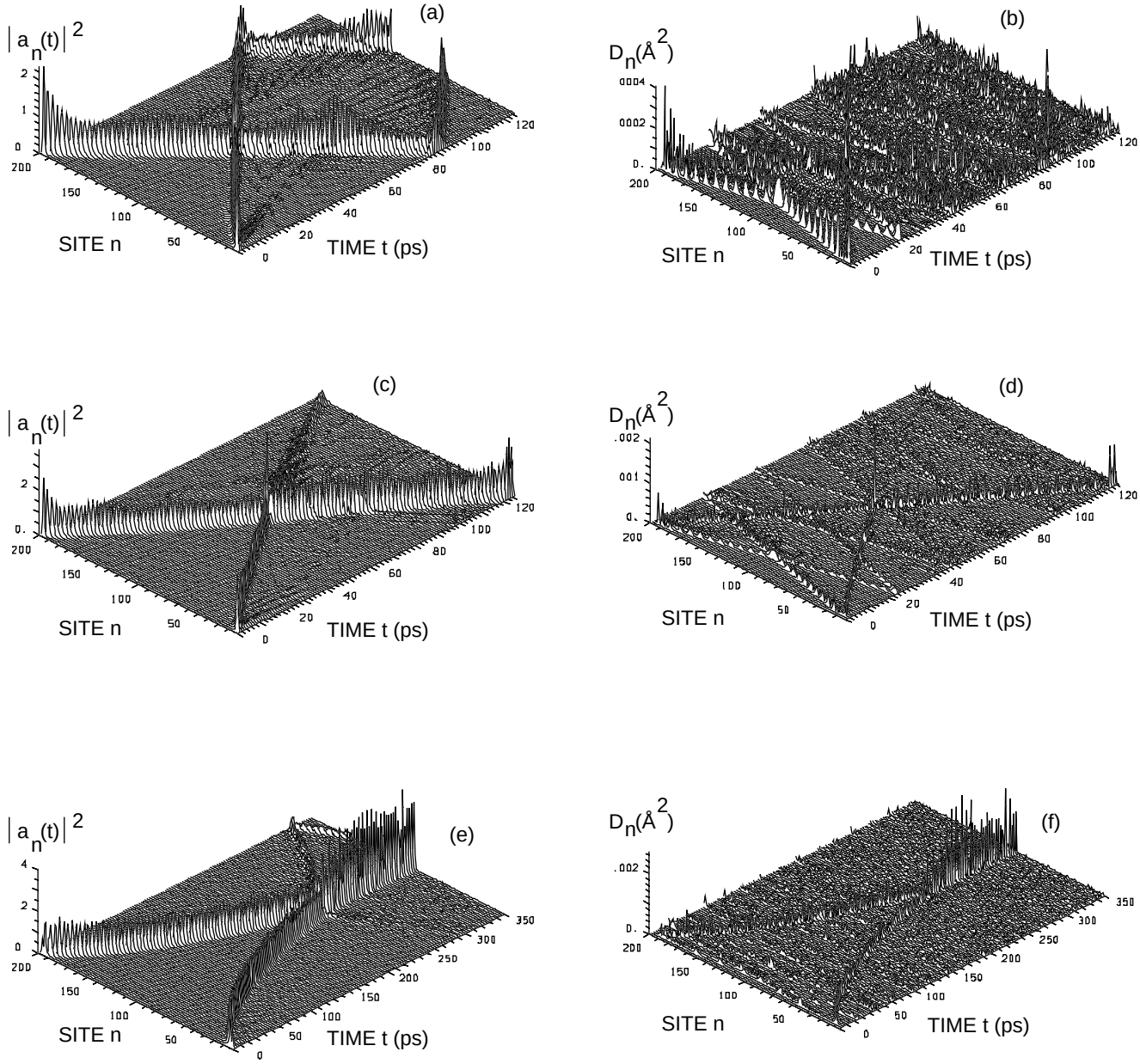

Figure 2. *The probability $|a_n|^2$ (a,c,e) and the squared local lattice deformation D_n (b,d,f) as functions of site n and time t for the time evolution of two amide-I quanta, initially localized close to the two chain ends (in equal fractions, i.e. $a_2(0) = a_{199}(0) = 1/2$) for J = 0.967 meV, W = 13 N/m and for three values of the coupling constant χ at T = 0 K for an open chain of 200 units with units 1 and 200 kept fixed during the simulations in the $|D_2>$ model (the time step size was 5 fs and a 4th order Runge-Kutta method was used).*

(a,b) χ = 50 pN (c,d) χ = 62 pN (e,f) χ = 75 pN

heat bath. Here Γ is the inverse time constant of the heat bath and thus an additional parameter, which is usually chosen as the lowest phonon frequency which for 200 units and standard parameters has a value of 0.2046/ps.

Our simulations indicate, that the two models behave similar. We performed simulations with the two models for several values of W and χ for a one-quantum excitation of the amide-I chain initially localized at one of the chain ends at 300K. The results for the model with thermal lattice population are shown in Figure3. We see that at 300K several thresholds appear. The threshold χ_1 between travelling solitons and dispersive cases in the left part of the panel agrees fairly well with the solid line, which represents the 0K threshold for soliton formation from continuum theory. Further we

find a second threshold (lower dashed line) χ_2. For $\chi > \chi_2$ the travelling solitons are destroyed by thermal fluctuations. Since χ_2 (W) intersects χ_1 (W) there is also a threshold value for W, W_t, below which no travelling solitons exist. In addition, a third threshold occurs, such that for $\chi > \chi_3$ pinned solitary waves occur. Physically for $W > W_t$ if $\chi < \chi_1$ the non-linearity is simply not strong enough to prevent the dispersion of the initial excitation. For $\chi_1 < \chi < \chi_2$ it is strong enough for this purpose and travelling solitons are formed. Since thermal fluctuations of the lattice enter the equations for the oscillators in a term proportional to χ, dispersion occurs again for $\chi_2 < \chi < \chi_3$. Then the fluctuations in $\chi(q_{n+1}-q_n)a_n$ are large enough to destroy the coherent structures. Finally for $\chi > \chi_3$ pinned solitons are formed due to the strong localizing effect of the non-linearity. W_t occurs because for small W, the displacements $(q_{n+1}-q_n)$ have to be large to accomodate a potential energy of $0.5(N-1)k_BT$ in the lattice phonons. These random displacements are then large enough to prevent the formation of coherent structures.

In conclusion, at T = 300 K solitons are only stable in the $|D_2>$ model if the force constant of the hydrogen bonds is larger than roughly 30–40 N/m at reasonable values of χ. However, the usually used value of W = 13 N/m is measured in crystalline formamide, where the formamide molecules can vibrate freely against each other in the potential due to the hydrogen bonds. In an α–helix on the contrary they are bound covalently in the backbone of the protein. Thus an effective force constant being larger than the formamide-value

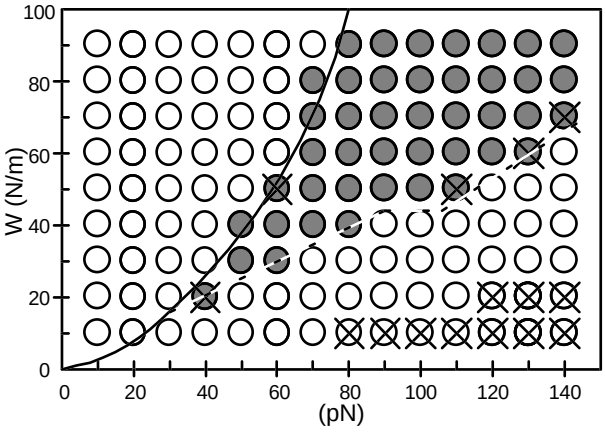

Figure 3. *Results of simulations for different values of W and χ for a one-quantum excitation of the amide-I chain, initially localized at one of the chain ends at 300K using the model with thermal lattice population and the $|D_2>$ ansatz. Each circle represents a simulation performed, where an open circle stands for a dispersive case, a hatched one for the formation of travelling solitons, a crossed open one for pinned solitons, and a crossed hatched one for travelling, slowly dispersing solitary waves. The solid line represents the threshold for soliton formation from 0K continuum theory.*

seems to be very probable. Preliminary *ab initio* calculations of W point also into this direction [39]. Further Bolterauer [10] and Cruzeiro-Hansson [36] could show, that in case of a classical system interacting with a quantum one as in our case, the classical system transfers a too large amount of energy to the quantum one, and thus simulations as discussed should underestimate soliton stability. However, besides these encouraging findings, there are also some more basic problems connected mainly with the semi-classical nature of the $|D_2>$ ansatz, which we have to discuss now.

Conceptual Deficiences

The semiclassical $|D_2>$ ansatz, discussed so far, has a couple of short-comings. First of all, as Cruzeiro et al. [33,34] point out, the state is an exact solution of the Schrödinger equation only if the Hamiltonian contains instead of momentum and displacement operators for the lattice only their real values $p_n(t)$ and $q_n(t)$, respectively. We have shown, that for the case of the Su-Schrieffer-Heeger Hamiltonian for polyacetylene a similar exact solution exists, if the momenta and displacements of the CH-units are taken as entirely classical [36]. Further, the semi-classical ansatz for the Davydov model cannot reproduce the known exact solution for special cases. $|D_2>$ yields correct solutions for the so-called decoupled case ($\chi = 0$), but not for the small polaron limit (J = 0) (see [31] for a discussion and for references). Further, Cottingham and Schweitzer [11] could show, that the complete Davydov Hamiltonian can be split into a part, which has a soliton of $|D_2>$ type as exact solution and a perturbation. Thus they could compute the life-time of a $|D_2>$-soliton when it is placed in the physical system of the complete Hamiltonian via time-dependent pertubation theory. They found that this type of solitons, derived from the $|D_2>$ ansatz (in the continuum model) decays into a delocalized exciton together with a set of phonons within a very short time. Thus one has to use an improved ansatz, to include quantum effects in the lattice into the theory. In their calculations they were also able [11] to include temperature effects.

However, Cruzeiro et al. [35, 36] could show that with the help of the $|D_2>$ ansatz one can estimate the quality of temperature models, because it is an exact solution of the above described reduced form of the Hamiltonian, and thus one can apply Monte-Carlo simulation methods to this classical form of the Hamiltonian. In this way Cruzeiro [36] could show numerically, that the Langevin method overestimates the effects of temperature and thus life-times at finite temperature as estimated with this method should be lower limits of the true life-time of solitons, however, again only for a system which would be described by the reduced form of the Hamiltonian. Thus on the one hand, the Langevin model overestimates effects of thermal fluctuations, while on the other hand the $|D_2>$ model as such overestimates the effects of the nonlinearity, since these are again consequences of a coupling between a classically described lattice and a quantum mechanically described oscillator system. The results of

Cottingham and Schweitzer [11] and the soluble special cases indicate that there are significant differences between the physics as described by the full Hamiltonian and those for the reduced form. Thus one has to search for an improved ansatz state.

The Quantum Mechanical $|D_1>$ Ansatz

The $|D_1>$ ansatz was introduced by Davydov [2, 3] for the inclusion of temperature effects. Unfortunately, as discussed above, Davydov obtained incorrect equations of motion for this ansatz. However, the probably most clear insight into the origin of this ansatz can be gained, if one looks at a formally exact solution of the Schrödinger equation which can be written in the form [16]:

$$|\psi> \;=\; \sum_n a_n(t)\hat{a}_n^+ e^{\hat{S}_n(t)}\,|0> \tag{19}$$

where the operator in the exponential contains only phonon operators and time-dependent complex parameters:

$$\hat{S}_n(t) \;=\; \sum_k \left(b_{nk}(t)\hat{b}_k^+ \;-\; b_{nk}^*(t)\hat{b}_k \right) \;+\; \sum_{k'k} f_{kk'n}(t)\hat{b}_k^+\hat{b}_{k'} \;+ \\ +\; \frac{1}{2}\sum_{k'k}\left(g_{k'kn}(t)\hat{b}_k^+\hat{b}_{k'}^+ \;-\; g_{k'kn}^*(t)\hat{b}_k\hat{b}_{k'} \right) + \ldots \tag{20}$$

To obtain the exact solution, all possible multi-phonon terms (up to infinite order) would have to be included into the operator. Thus as a first step in the improvement of ansatz states it is quite natural to retain only the one-phonon terms in the expansion given above, and to neglect all multi-phonon interactions. This leads to the $|D_1>$ ansatz as discussed below.

Equations of Motion

Thus the $|D_1>$ ansatz for $|\psi>$ can be written in the form

$$|D_1> \;=\; \sum_n a_n(t)\hat{U}_n\hat{a}_n^+\;|0> \tag{21}$$

where the coherent state operators are given by

$$\hat{U}_n\,|0>_p = \exp\left[-\frac{1}{2}\sum_k |b_{nk}(t)|^2\right]\cdot\exp\left[\sum_k b_{nk}(t)\hat{b}_k^+\right]|0>_p \\ = \exp\left\{\sum\left[b_{nk}(t)\hat{b}_k^+ - b_{nk}^*(t)\hat{b}_k\right]\right\}|0>_p \tag{22}$$

Note, that the second equality again holds only if the operator acts on the phonon vacuum $|0>_p$, and that in our notation $|0> = |0>_e|0>_p$, where $|0>_e$ is the vacuum state for the amide-I oscillators (exciton vacuum). Physically, this ansatz allows that amide-I oscillators in different excitation states can excite different numbers of phonons in the lattice according to their excitation probability.

The equations of motion for these quantities can again be obtained with the Euler-Lagrange equations of the second kind [6, 14, 15, 19,22,27–30]. Note, that with the Hamiltonian method in the form used previously by Davydov and others, incorrect equations are obtained in case of the $|D_1>$ state [19]. The final equations of motion for the $|D_1>$ ansatz are

$$i\hbar\,\dot{a}_n = -\frac{i\hbar}{2}\sum_k\left(\dot{b}_{nk}b_{nk}^* - \dot{b}_{nk}^* b_{nk}\right)a_n + \\ +\sum_k \hbar\omega_k\left[B_{nk}\left(b_{nk}+b_{nk}^*\right)+|b_{nk}|^2\right]a_n - \\ - J\left(D_{n,n+1}a_{n+1} + D_{n,n-1}a_{n-1}\right) \tag{23}$$

$$i\hbar\,\dot{b}_{nk} = \hbar\,\omega_k\left(b_{nk}+B_{nk}\right) - J\left[D_{n,n+1}\left(b_{n+1,k}-b_{nk}\right)\frac{a_{n+1}}{a_n} + \right. \\ \left. + D_{n,n-1}\left(b_{n-1,k}-b_{nk}\right)\frac{a_{n-1}}{a_n}\right]$$

where the coherent state overlaps are given by

$$D_{nm} = \exp\left[-\frac{1}{2}\sum_k\left(|b_{nk}-b_{mk}|^2 + b_{nk}b_{mk}^* - b_{nk}^*b_{mk}\right)\right] \tag{24}$$

Mechtly and Shaw [18] have shown, that for initial conditions $a_n(0) = \delta_{n1}$ and $b_{nk}(0) = 0$ the small time behaviour of the system poses no difficulties due to the denominators $a_n(t)$ in eq. (26), although if they vanish for t approaching zero (see also [15] for details). To avoid numerical instabilities we follow the suggestion given in [18] and all a_n which vanish in the initial state are put to $a_n(0) = x$, where x is a small, physically insignificant number, e.g. x=0.005 [18]. Then the initial state is renormalized to 1. In our calculations we tried values of x between $5\cdot10^{-3}$ and $5\cdot10^{-10}$ without any visible change in the dynamics obtained, at least at 0 K temperature. Thus we used always x = 0.005 in our T = 0 K simulations. However, at 300 K (see below) we found that the results converge only with decreasing x, if x is chosen much smaller, i.e. $x=1\cdot10^{-8}$. For the numerical solution of the equations we used again a Runge-Kutta method, correct up to the fourth order in the size of the time step.

Quality of Results

It is now of utmost importance to find a measure which gives information to what extend exact dynamics are reproduced by the $|D_1>$ ansatz. One such tool is the investigation of special cases for which the time-dependent Schrödinger equation can be solved exactly [14]. One such case is the decoupled one, i.e. $\chi = 0$. In this case we have just the free oscillator system without any perturbation caused by the (also) free phonon system which is still present. The other special case is the so-called small polaron limit, where J = 0. Here we have an immobile amide-I excitation (vibrational exciton) which polarizes the lattice via the exciton-phonon interaction. It can be shown [14, 16, 18, 32], that in both cases the $|D_1>$ ansatz leads to a time evolution of the state which satisfies the time-dependent Schrödinger equation, both analytically and also in numerical simulations [14].

Further, it was shown [18] in general that for the $|D_1>$ state

$$< D_1(t)|\ i\hbar\frac{\partial}{\partial t} - \hat{H}\,|D_1(t)> \ = \ 0 \tag{25}$$

holds, but

$$\left(i\hbar\tfrac{\partial}{\partial t} - \hat{H}\right)|D_1(t)> = J\,|\delta(t)>$$

$$\begin{aligned}|\delta(t)> = -\sum_n \Big\{ & a_{n+1}\left(D_{n,n+1}|\beta_n> - |\beta_{n+1}>\right) - \\ & - a_{n-1}\left(D_{n,n-1}|\beta_n> - |\beta_{n-1}>\right) + \\ & + \sum_k \Big[a_{n+1}\left(b_{n+1,k} - b_{nk}\right)D_{n,n+1} + \\ & + a_{n-1}\left(b_{n-1,k} - b_{nk}\right)D_{n,n-1}\Big]\cdot \hat{U}_n \hat{b}_k^+\,|0>_p \Big\} \hat{a}_n^+\,|0>_e\end{aligned} \tag{26}$$

where $|\beta_n> = \hat{U}_n(t)\,|0>_p$ is the coherent state at site n. With the help of the state vector $|\delta(t)>$ as given above and the dimensionless state vector $|\lambda(t)> = \left(\hat{H}/J\right)|D_1(t)>$ we derived expressions for the expectation values [29]

$$\begin{aligned}&< \gamma|\gamma >,\ < \gamma|\hat{a}_n^+\hat{a}_n|\gamma >,\ < \gamma|\hat{b}_k|\gamma > \\ &< \gamma|\hat{p}_n|\gamma >,\ < \gamma|\hat{q}_n|\gamma >,\ < \beta_{nk}|\gamma > \\ &\qquad |\gamma > \ = \ |\delta >,\ |\lambda >\end{aligned} \tag{27}$$

These expectation values could be calculated during $|D_1>$ simulations and compared with each other. We found that for all of them the expectation values invoking the deviation state were orders of magnitude smaller than those with $|\lambda>$ for times between a few ps up to 10 ns [15]. Further we studied the very small time behaviour of $|D_1>$ in comparison to a Taylor expansion in time of the exact solution for the Davydov Hamiltonian in our previous paper [15] and found again satisfactory agreement between them. From these results we concluded, that the $|D_1>$ ansatz recovers the exact dynamics of the systems quantitatively with very small errors. Thus one can trust results which are obtained with the help of the $|D_1>$ ansatz.

Initial States and Applications

First of all it is of utmost importance to compute initial values $b_{nk}(0)$ from a given set of initial lattice momenta $p_n(0)$ and distortions $q_n(0)$. Unfortunately, while there exists a unique relation to compute momenta and distortions from a given set of coherent state amplitudes, for the reverse situation this is not the case. Thus we concentrate on the exactly soluble special cases [32] to deduce informations on the form of the initial state from these. Indeed this is possible: it turns out, that the initial coherent state amplitudes have to be site-independent if the $|D_1>$ ansatz should yield the correct solution. The site-dependence of the b_{nk}'s has to evolve through the equations of motion. Fortunately for this case a unique relation exists [14]:

$$b_{nk}(0) = \sum_{n'}\left[\sqrt{\frac{M\omega_k}{2\hbar}}\,U_{n'k}\,q_{n'}(0) + \frac{i}{\sqrt{2\hbar M\,\omega_k}}\,U_{n'k}\,p_{n'}(0)\right] \tag{28}$$

Note, that this holds also, if $|D_1>$ like ansätze should be used to describe dynamics of poly-acetylene chains in the Su-Schrieffer-Heeger model, in contrast to our previous suggestion [40].

We have found that in the $|D_1>$ case, in contrast to $|D_2>$, a strong dependence of the dynamics on the initial excitation site exists. Using the usual parameter values, we found, that from an initial excitation at the chain end where the C=O group is directly coupled to the lattice solitons appear at 0K for the usual values of the parameters. Indeed, if the amide-I system is excited initially at that end (oscillator no. 1 in our case) of the chain the appearance or disappearance of solitons as function of χ is very similar to the corresponding $|D_2>$ case. However, if we excite initially at the other chain end, where the C=O group is not directly coupled to the lattice, solitons are only formed if roughly $\chi > 170$ pN, a value much too large to be reasonable. To illustrate this, we show in Figure 4 the dynamics of the amide-I excitations for these two cases in a chain of 51 units. In the case of an initial excitation somewhere within the chain we find solitons again only at very large values of the coupling constant (roughly $\chi >$

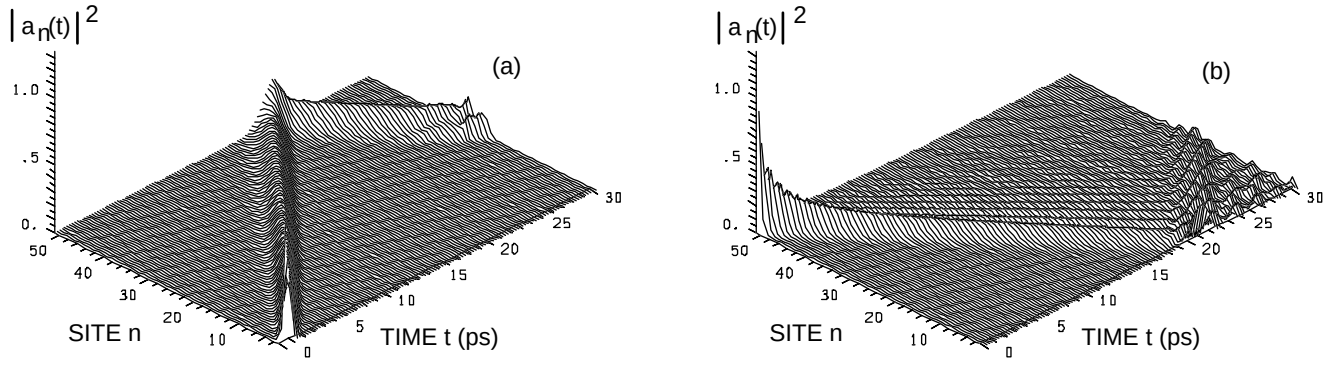

Figure 4. *The probability $|a_n|^2$ to find an amide-I quantum as function of site n and time t for the time evolution of one amide-I quantum, initially localized (n_0) at different chain ends for J = 0.967 meV, W = 13 N/m and χ = 60 pN at T = 0 K for an open chain of N = 51 units in the $|D_1>$ model (4^{th} order Runge-Kutta method with 200,000 time steps of a size of 0.15 fs; $x=1\cdot10^{-8}$).*
(a) $n_0=1$ (b) $n_0=51$

170 pN). This could be due to the shock waves in the lattice interacting with the wave-trains or to interactions of the two trains with each other, after one is reflected from the chain end closer to the initial excitation site. However, a possible reason for this feature is also, that in this case from the initial excitation site two wave trains in opposite direction are emitted, and thus each of them carries only half of an amide-I quantum. From $|D_2>$ dynamics we know, however, that a reduced number of quanta carried destabilizes solitons. The equations of motion for multi-quanta $|D_1>$ states are far more complicated than for the $|D_2>$ case and simulations with such states have not been performed so far, at least to our knowledge. We have derived the necessary equations, but we haven't programmed them yet. Basically the conclusion for 0 K is, that we can expect the formation of Davydov solitons only if the initial excitation occurs at one well defined chain end, namely that one, where the C=O unit is coupled to the lattice. Now we have to turn to the influence of temperature on the dynamics.

Temperature Effects

In principle we have also in this case the possibility to populate the lattice with a thermal phonon distribution prior to the initial amide-I excitation. However, it turned out that in $|D_1>$ theory this is not a reasonable procedure to account for temperature effects. Davydov used an averaged Hamiltonian method which starts from an initial state containing an arbitrary phonon distribution together with a unitary operator $\hat{U}_n$ of the lattice displacements (note, that in this case the two forms of a coherent state as discussed above for the T = 0 K case are no longer equivalent)

$$|D_1,\nu> = \sum_n a_n(t)\hat{a}_n^+\hat{U}_n|\nu>$$

$$\hat{U}_n = \exp\left[\sum_k\left(b_{nk}(t)\hat{b}_k^+ - b_{nk}^*(t)\hat{b}_k\right)\right] \qquad (29)$$

where the arbitrary distribution of quanta on the different normal modes is given by

$$|\nu> = \prod_k \frac{\left(\hat{b}_k^+\right)^{\nu_k}}{\sqrt{\nu_k!}}|0> \qquad (30)$$

Then a thermally averaged (over all possible distributions) Hamiltonian is formed:

$$H(T) = \sum_{n\nu}\rho_\nu(T)<D_1,\nu|\hat{H}|D_1,\nu>$$

$$\rho_\nu(T) = \frac{f_\nu(T)}{\sum_\mu f_\mu(T)} \quad ; \quad f_\nu(T) = <\nu|e^{-\frac{\hat{H}_p}{k_BT}}|\nu> \qquad (31)$$

where $\hat{H}_p$ is the phonon part of the Hamiltonian, and k_B is Boltzmann's constant. Then from a thermally averaged Lagrangian equations of motion for the a's and b's are derived. The resulting equations of motion are rather lengthy, and given in detail in [22]. Therefore we do not repeat them here, but present the necessary equations in Appendix A, mainly because the complete derivation was never presented in the literature, only the final results in [17], unfortunately calculated with Davydov's version of Hamilton's principle, which yields incorrect equations of motion.

In the literature Quantum Monte Carlo (QMC) results on the Davydov model with cyclic boundary conditions and a symmetric interaction at different temperatures can be found [23]. After introducing these features into our program, we

could perform time simulations with exactly the same physical parameters. At the same temperature as Wang et al. [23], we found formation of solitons, and at somewhat larger temperatures, we could reproduce a change from coherent structures to Anderson localized states using the averaged Hamiltonian method. Thus we conclude that this method yields qualitatively the same results as the QMC simulations [23]. However, an averaged expectation value, computed in [23], the model is not able to reproduce. Therefore we view Davydov's model as an approximation which yields qualitatively (soliton formation or not) the correct results, but is quantitatively not correct. The lattice population model yields even qualitatively wrong results. In the next section we give a short description, in which way we want to overcome the problems associated with Davydov's model, which can even be critisized from a statistical mechanics point of view.

In simulations it turned out to be quite important, that in the averaged Hamiltonian method a factor appears at the dispersion terms, containing a real part which is exponentially decreasing with increasing temperature. This factor decreases the dispersive character of the system: it can enhance localization (immobile) due to disorder of the Anderson type. Thus the effective dispersion parameter *J* is reduced with increasing temperature. This leads to the result, that at 300 K we usually obtain solitons for parameters which yield a dispersive behaviour at 0 K, while at parameter-values, where travelling solitons are found at 0 K, at 300 K mostly pinned excitations form which most probably are Anderson localized states. Thus the solitary waves found in our calculations at T = 300 K result from a delicate interplay between the nonlinearity, which leads to localization in a coherent manner, the dispersion, which tends to delocalize the excitation or makes it mobile, and Anderson localization due to disorder, originating from thermal fluctuations, which tends to lattice pinning of the excitation. In Figure 5 we show in the same way as above the results of our survey of the parameter space for an initial excitation at the chain end where the CO group of the unit is not directly coupled to the phonon system. Note that in this case we found only dispersing behaviour up to large values of the nonlinearity at T = 0 K.

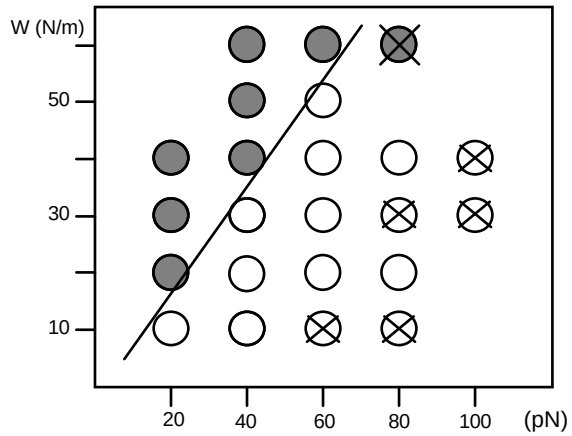

Figure 5. *Results of simulations for different values of W and χ for a one-quantum excitation of the amide-I chain, initially localized at that one of the chain ends which is not directly coupled to the phonon system (N = 50, n_0 = 49), at 300 K using Davydov's averaged Hamiltonian model for the $|D_1>$ state. Each circle represents a simulation performed, where an open circle stands for a dispersive case, a hatched one for the formation of travelling solitons, a crossed open one for pinned solitons, an open one with a point for a localized, slowly dispersing excitation, and a crossed hatched one for travelling, slowly dispersing solitary waves.*

Figure 5 indicates that again we find travelling solitons only for values of W being larger than roughly 30–40 pN and at reasonable values of the nonlinearity. However, now these solitons need not to be started from that end of the chain where the C=O group is directly coupled to the phonon system. Note, that for 300 K, solitons can be excited not only from the terminal unit itself, but also from the unit left of the terminal one inside the chain, however, not from the second-left one, where two slowly dispersing waves are formed, i.e. for N = 51, solitons can be formed from units 51 and 50, but not from 49. However, at T = 300K also when starting the simulation with an excitation at the other chain end, namely from initial excitation sites 1 or 2 solitary waves are found, while in the centre of the chain only slowly dispersing solitary waves can be seen. In Figure 6 we display some examples for such solitons and solitary waves, also for different chain lengths. However, as Figure 6 indicates there are also cases, where from the initial excitation first of all a slowly dispersing solitary wave is emitted. Afterwards, the excitation is accumulated again at the chain end due to Anderson localization. When, after some time the excitation probability is large enough, again a solitary wave travels through the chain (Figure 6d). Obviously the solitons appearing at 300 K are able to pass once through the chain, no matter how long it is, but they start to disperse after collision with the chain end. An interesting feature of our model is, that the solitons at 300 K in a system of three coupled (by transition dipole moments of the C=O groups) chains (as it is the case in an α–helix) are of similar stability as in the case of one isolated chain. In Figure 7 we show four different examples of that case. As the Figure shows, in the three-chain case the solitons have a quite complicated structure, with fractions of the amide-I quantum oscillating between different chains. Thus we can conclude, that at reasonable parameter values also at 300 K solitons are only stable if they are initiated from one of the chain ends and its next neighbor. However, solitary wave like features, in some cases occurring only after reflections at chain ends are found in each case.

Improvements

Since the averaged Hamiltonian is only qualitatively correct, we attempted [15, 32] to expand the formally exact solution

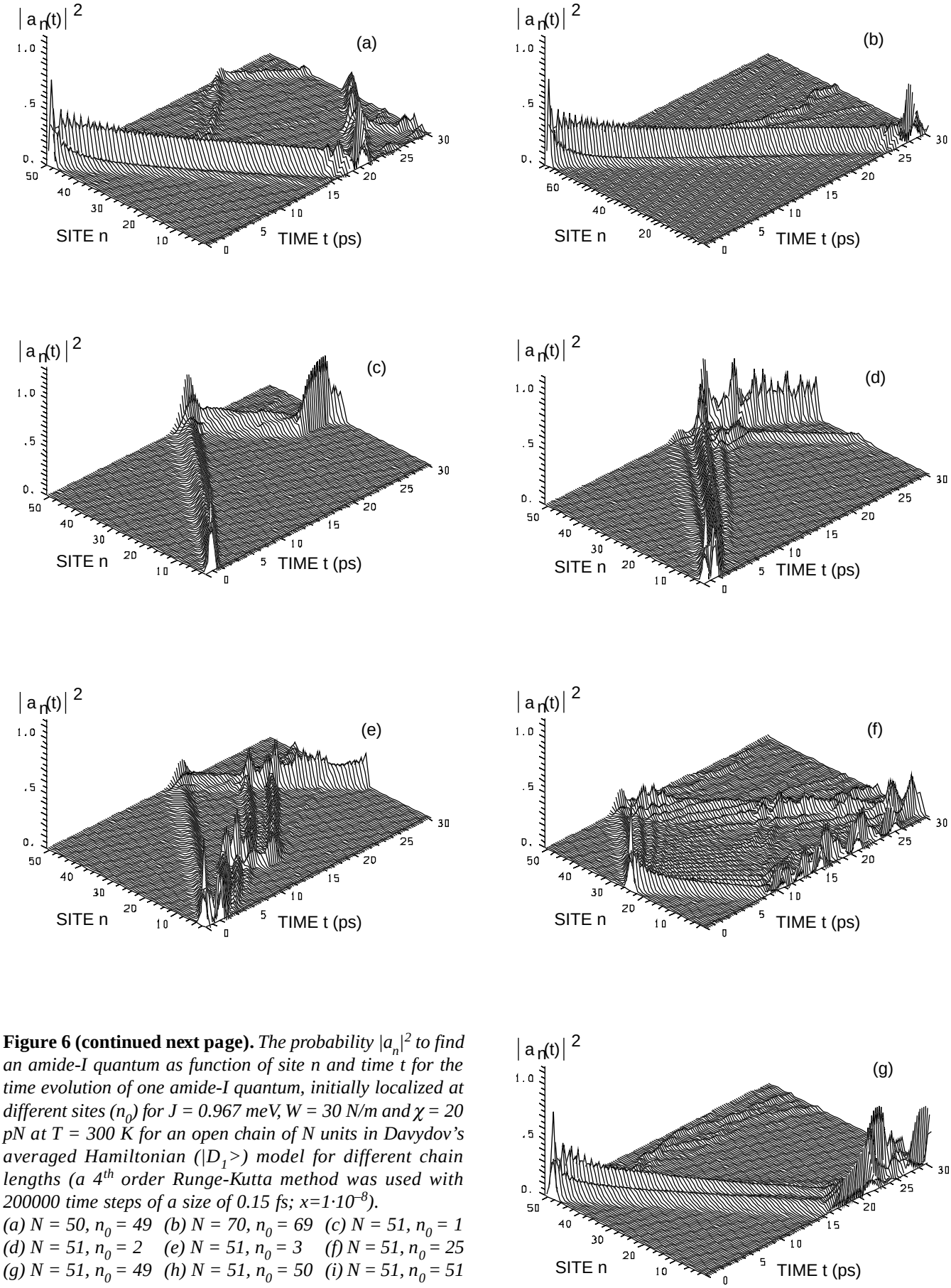

Figure 6 (continued next page). *The probability $|a_n|^2$ to find an amide-I quantum as function of site n and time t for the time evolution of one amide-I quantum, initially localized at different sites (n_0) for J = 0.967 meV, W = 30 N/m and χ = 20 pN at T = 300 K for an open chain of N units in Davydov's averaged Hamiltonian ($|D_1>$) model for different chain lengths (a 4th order Runge-Kutta method was used with 200000 time steps of a size of 0.15 fs; x=1·10^{-8}).*
(a) N = 50, n_0 = 49 (b) N = 70, n_0 = 69 (c) N = 51, n_0 = 1
(d) N = 51, n_0 = 2 (e) N = 51, n_0 = 3 (f) N = 51, n_0 = 25
(g) N = 51, n_0 = 49 (h) N = 51, n_0 = 50 (i) N = 51, n_0 = 51

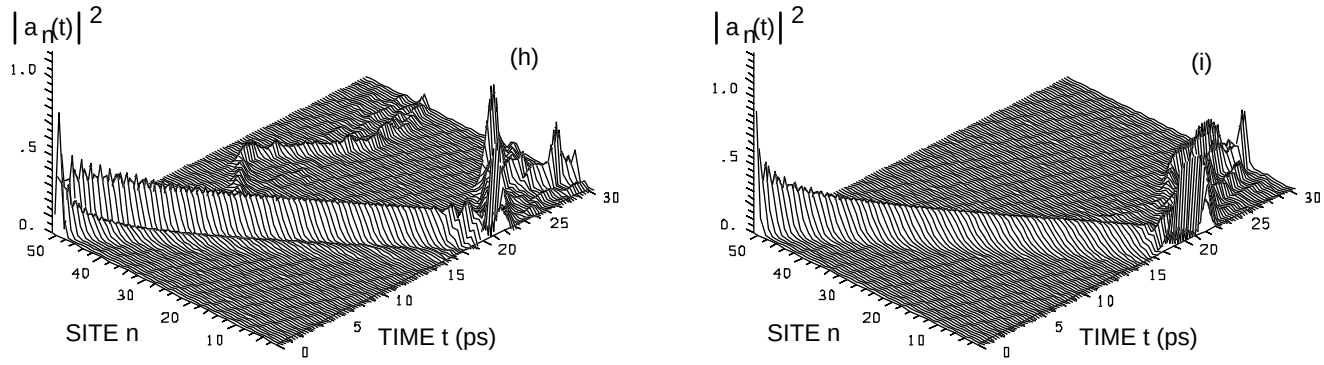

Figure 6 (continued).

$$|\psi(t)> \;=\; e^{-\frac{i}{\hbar}\hat{H}t}\,|\psi(0)> \qquad (32)$$

of the Schrödinger equation in a power series in time, in order to obtain exact dynamics at least for very short time and to compare them with $|D_1>$ results [15]. We found that $|D_1>$ seems to be correct not only on larger time scales, but also in the range of a few tenth of a picosecond, i.e. the time, when the lattice distortion necessary to form a soliton just develops [15]. However, we could sum up some terms in the expansion to infinite order in time. This should lead to a propagation method for the computation of the dynamics. Namely, one could use these infinite order terms for a small time step, and then use the result again as initial excitation for the next time step, for which one could use again the infinite order terms acting on the new initial state and so forth. Such a program could lead to a more straightforward method to incorporate temperature into the theory. First of all one could use similar procedures, to obtain infinite order terms for a lattice, which is initially excited as in Davydov's averaged Hamiltonian method. However, in this case one would not need to derive equations of motion from a thermally averaged Lagrangian (which as mentioned is a quite questionable procedure), but one could obtain for short time steps and a given phonon distribution analytical wave functions. From these one could compute expectation values of the operators of interest (e.g. number operators for the amide-I oscillators, phonon operators and consequently momenta and displacements). Since these expectation values would be given also analytically, one probably could perform a thermal average on them and in this way obtain reliable dynamics [15].

Computation of Spectra

As outlined in the above sections, solitons have been found theoretically within the Davydov model at reasonable parameter values and at all temperatures up to 300 K. Thus the question arises why in the infrared spectra of the amide-I band in polypeptides [42] no unusual features were found experimentally which could be attributed to solitons. Thus we computed spectra from our dynamical simulations for such cases where solitons are formed, and others which show dispersive behaviour. This is necessary, in order to decide whether the experimental failure to find solitons in the spectra is a proof for their absence or not. As worked out e.g. in the paper by Heller [43], from dynamic simulations one can calculate directly the usual form of an absorption cross section with the help of the auto-correlation function S(t) (a_0 is Bohr's length and á the fine structure constant)

$$\sigma(\omega) \;=\; 8\pi^2\alpha a_0^2\omega\int_0^{t_S}\mathrm{Re}\left[e^{\frac{i}{\hbar}Et}S(t)\right]dt \qquad (33)$$

In principle we have here a full Fourier transformation (integration over $-\infty < t < \infty$) of $\exp[iEt/\hbar]S(t)$, however, since $S(-t) = S^*(t)$ we can restrict the integration to a half transormation of the real part of the argument. This holds, because $S(-t) = <\varphi(0)|\varphi(-t)> = <\varphi(0)|\exp\left[it\hat{H}/\hbar\right]|\varphi(0)>$ $= <\varphi(t)|\varphi(0)> = \left(<\varphi(0)|\varphi(t)>\right)^* = S^*(t)$. In eq. (33) we have $E = E_i + \hbar\omega$, where ω is the frequency of the incident radiation and E_i is the energy of the initial state prior to the amide-I excitation, i.e. in the T = 0 K case the vacuum. This is necessary to set the energy scale of the incident radiation correctly. The resolution becomes the better, the longer the simulation time t_S (which in principle should be infinite) is, up to which the integration is performed. We take as starting state at T = 0 K simply our lattice with only the zero-point vibration excited. Thus we obtain for $S(t)$ simply

$$S(t) = <\varphi(t=0)|\varphi(t)> \;;\quad E_i = \frac{1}{2}\sum_k \hbar\omega_k \qquad (34)$$

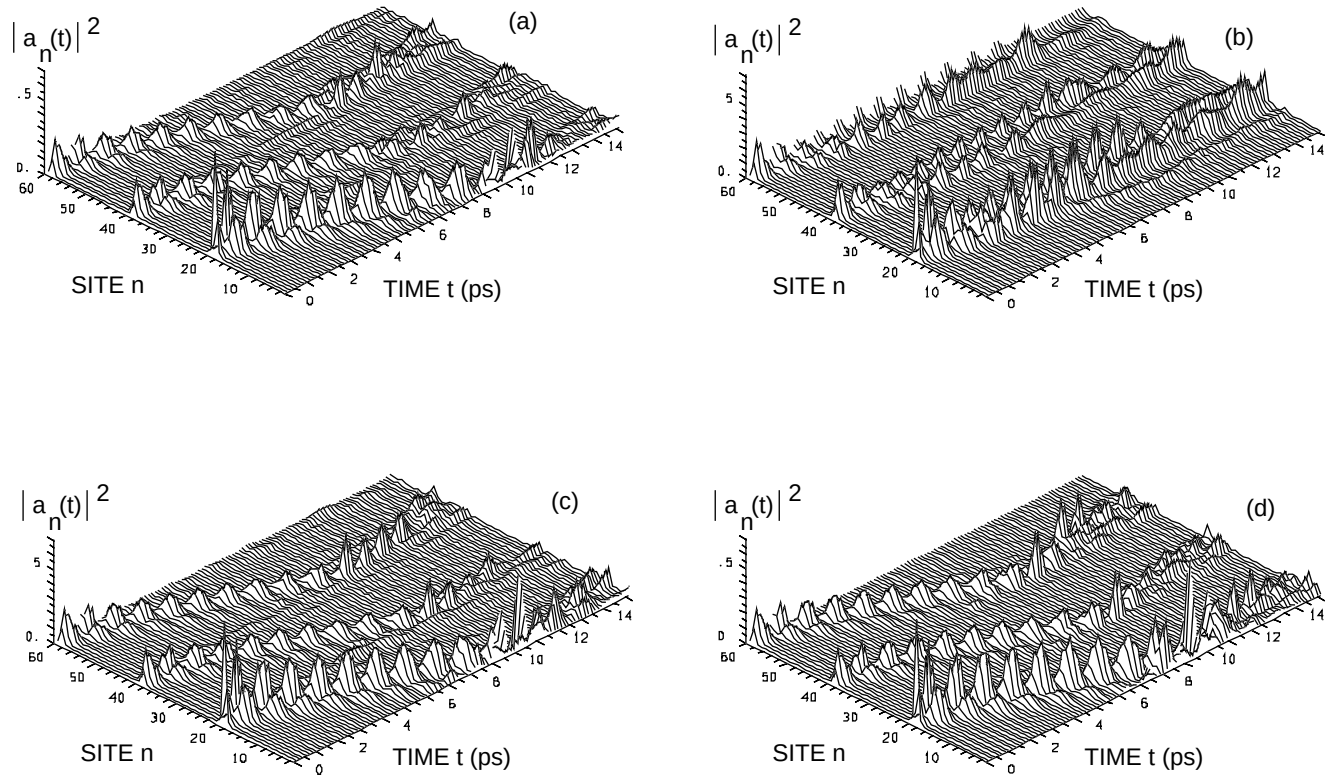

Figure 7. *The probability $|a_n|^2$ to find an amide–I quantum as function of site n and time t for the time evolution of one amide–I quantum in a system of three coupled chains (first chain: n = 1–20, second chain: n = 21–40, third chain n = 41-60), initially localized at that end of the first chain which is not directly coupled to the phonon system for J = 0.967 meV at T = 300K using Davydov's averaged Hamiltonian ($|D_1>$) model for different values of the spring constant W of the hydrogen bonds and of the nonlinearity (the next–neighbor interchain dipole coupling constant is 1.5373 meV, following Scott [1]; 4th order Runge–Kutta method with time steps of a size of 0.1 fs; x = 0.005 was used here, because for the usual $x = 1 \cdot 10^{-8}$ the error in total energy increases by 7 to 8 orders of magnitude, although to only 10^{-6} eV, after roughly 1 ps, indicating most probably numerical difficulties with the denominators in the equations of motion).*
(a) W = 19 N/m, χ = 35 pN (b) W = 20 N/m, χ = 62 pN
(c) W = 40 N/m, χ = 62 pN (d) W = 60 N/m, χ = 62 pN

E_i is the energy of the groundstate (as mentioned, the vacuum), while $|\varphi(t=0)>$ is the excited initial state $|\varphi(t=0)> = \mu_{if}|\chi_i>$ ($|\chi_i> = |0>$ here and $|\varphi(t=0)> = \Sigma_n a_n(0)\hat{a}_n^+|0>$) and μ_{if} the transition dipole moment operator between initial state i and final state f. The ecitation energy of 0.205 eV is already contained in the phase factor of the total wave function, while the zero point energy is included in E_i to set the correct scale for the energy of the incident radiation.

Therefore

$$|\varphi(t)> = e^{-\frac{it}{\hbar}\left[E_0+\frac{1}{2}\sum_k \hbar\omega_k\right]} \sum_n a_n(t) e^{-\frac{1}{2}\sum |b_{nk}(t)|^2} \cdot e^{\sum_k b_{nk}(t)\hat{b}_k^+} \hat{a}_n^+ |0> \qquad (35)$$

and thus

$$S(t) = e^{-\frac{it}{\hbar}\left[E_0+\frac{1}{2}\sum_k \hbar\omega_k\right]} \sum_n a_n^*(0) a_n(t) < 0|\beta_n(t)> \qquad (36)$$

where:

$$|\beta_n(0)> = |0> \quad ; \quad <0|\beta_n(t)> = e^{-\frac{1}{2}\sum_k |b_{nk}(t)|^2}$$

The time integration is performed during the simulation using a simple Simpson scheme. In case of the averaged Hamiltonian method for finite temperatures we use as initial state one with thermally populated normal modes:

$$E_i = \sum_k \hbar\omega_k \left(\nu_k + \frac{1}{2}\right); \quad \nu_k = \left[\exp\left(\frac{\hbar\omega_k}{k_B T}\right) - 1\right]^{-1} \tag{37}$$

In order to be consistent with the averaged Hamlitonian, we form an averaged autocorrelation function with the state

$$|\varphi_{ny}(t)> = e^{-\frac{it}{\hbar}\left[E_0 + \sum_k \hbar\omega_k\left(\nu_k + \frac{1}{2}\right)\right]} \cdot \cdot \sum_n a_n(t)\, e^{\sum_k \left[b_{nk}(t)\hat{b}_k^+ - b_{nk}^*(t)\hat{b}_k\right]} \hat{a}_n^+ |\nu> \tag{38}$$

Thus we have the thermally averaged correlation function

$$S(t) = e^{-\frac{it}{\hbar}\left[E_0 + \sum_k \hbar\omega_k\left(\nu_k + \frac{1}{2}\right)\right]} \cdot \sum_n a_n^*(0) a_n(t) \cdot \cdot \sum_\nu \rho_\nu <\nu|\hat{U}_n^+(0)\hat{U}_n(t)|\nu> \tag{39}$$

The expectation value in $S(t)$ can be easily written down by noticing that the thermally averaged overlap between two coherent states at different sites is given by ([17] and in Appendix A)

$$D_{nm}(t) = \sum_\nu \rho_\nu <\nu|\hat{U}_n^+(t)\hat{U}_m(t)|\nu> = = \exp\left\{\sum_k \left[(\nu_k + 1) b_{nk}^* b_{mk} + \nu_k b_{nk} b_{mk}^* - \left(\nu_k + \frac{1}{2}\right)\left(|b_{nk}|^2 + |b_{mk}|^2\right)\right]\right\} \tag{40}$$

From this our desired expectation value is obtained simply by introducing for b_{nk} the values $b_{nk}(0) = 0$ and for b_{mk} the values $b_{nk}(t)$ into the right hand side of the above equation. Thus

$$\sum_\nu \rho_\nu <\nu|\hat{U}_n^+(0)\hat{U}_n(t)|\nu> = = \exp\left[-\sum_k \left(\nu_k + \tfrac{1}{2}\right)|b_{nk}(t)^2\right] \tag{41}$$

and finally

$$S(t) = e^{-\frac{it}{\hbar}\left[E_0 + \sum_k \hbar\omega_k\left(\nu_k + \frac{1}{2}\right)\right]} \cdot \cdot \sum_n a_n^*(0) a_n(t) \exp\left[-\sum_k \left(\nu_k + \tfrac{1}{2}\right)|b_{nk}(t)|^2\right] \tag{42}$$

Note, that our phonon-states, formed with the help of the unitary displacement operator, $\hat{U}_n|\nu>$ are not eigenstates of the phonon annihilation operators, while $\hat{U}_n|0>$ is. On the contrary, such an eigenstate cannot be constructed in this way from $|\nu>$, because the basis space of oscillator states is not complete, when starting the expansion from $|\nu>$. However, we could find a solution of the equation (without loss of generality we give the equations just for the case of only one oscillator)

$$\hat{b}|\beta, \nu> \; = \; b(t)|\beta, \nu> \; + \; X(t)\,|\nu - 1>$$

ansatz:

$$|\beta, \nu> = \sum_{\mu=0}^{\infty} c_\mu \, |\mu + \nu> = = \sum_{\mu=0}^{\infty} c_\mu \sqrt{\frac{\nu!}{(\mu+\nu)!}} \left(\hat{b}^+\right)^\mu \, |\nu> \tag{43}$$

which would lead after normalization to

$$|\beta n, \nu> = \hat{U}_\nu \, |0>$$

$$\hat{U}_\nu = R_\nu(t)\left[e^{b(t)\hat{b}^+} - \sum_{\lambda=0}^{\nu-1} \frac{[b(t)]^\lambda}{\lambda!}\left(\hat{b}^+\right)^\lambda\right] \tag{44}$$

with

$$R_\nu(t) = e^{-i\nu\varphi(t)}\left[e^{|b(t)|^2} - \sum_{\eta=0}^{\nu-1} \frac{|b(t)|^{2\eta}}{\eta!}\right]^{-1/2} \tag{45}$$

where (t) is the phase of $b(t)$: $b(t)/b^*(t) = \exp[2i\varphi(t)]$ and $X(t)$ has to be

$$X(t) = \begin{cases} \dfrac{b^\nu(t)}{\sqrt{(\nu-1)!}} R_\nu(t) & ; \quad \text{if } \nu \geq 1 \\ 0 & ; \quad \text{if } \nu = 0 \end{cases} \tag{46}$$

For our ansatz state a similar relation holds:

$$\hat{b}_k \hat{U}_n(t)|\nu> = b_k(t)\hat{U}_n(t)|\nu> + \sqrt{\nu_k}\,\hat{U}_n(t)|\nu-1>_k$$
$$|\nu> = \prod_k |\nu_k> \;;\; |\nu-1>_k = \prod_{k'} |\nu_{k'} - \delta_{k'k}> \qquad (47)$$

where each $|\nu_k>$ represents the occupation of the normal mode k.

Examples of the calculated spectra are shown in Figure 8. As it is to be expected, solitons cannot be seen in the spectra at T = 0 K, because the Frank-Condon factor between an excitonic and a solitonic state for acoustical phonons in the Davydov model for proteins is extremely small (see [1] for a discussion). Only we observe that for larger nonlinearities, (Figure 8a) the fine structure of the amide-I band is more complicated than for free dispersion (not shown). When a soliton is formed, the band becomes a little bit more structured (Figure 8b) than in the case of nearly free dispersion. Furthermore a very small shoulder appears on the higher energy side of the amide-I band, which is absent at higher temperatures, but increases in intensity with increasing nonlinearity. At present we are not able to give a clear physical explanation for this feature. However, this shoulder is probably far too small in intensity to be observable. In conclusion, this observation fits to experiments on oligo-peptides [42] at low temperatures, where no special features in the spectra of the amide-I region were found, which might be attributable to solitons. Unfortunately in [42] no details are given for the high temperature behaviour of the amide-I band in peptides, but the discussion given there indicates that also at higher temperatures no unusual features are found. Also our results (Figure 8c) show, that although there is a soliton present in the system, it cannot be traced in the spectrum. Thus, even when Davydov solitons of the conventional type (amide-I mode coupled to acoustical phonons) are formed in the system under investigation (as in Figure 8b,c,d), they cannot be observed by the usual spectroscopic methods. Therefore, the experimental finding that the amide-I band in proteins shows no unusual features [42] cannot be used as a proof for the absence of Davydov solitons in the system. Thus one has to search for other experimental tools to detect solitons experimentally, e.g. the pump-probe experiments as suggested by Knox et al. [44].

However, the centre of the band is always shifted proportional to the nonlinearity factor χ. In Figure 8b at 0 K for χ = 60 pN this shift amounts to approximately 8 cm^{-1}. Probably, using well-defined α–helical samples such a shift could be used to obtain an experimental measure of χ, although the shift is quite small and might become undetectable when the band broadens at high temperatures. Note, that negative values of the intensities in the spectra indicate, that the total simulation time is not completely sufficient, or that some damping factor should be included in the exponential factor multiplied with $S(t)$ in the integrand.

As Figure 8d and e show, the amide-I band becomes splitted, when the initial excitation is not placed at the terminal site, but in its neighborhood. This phenomenon occurs here in systems where solitons are present. Further, the same

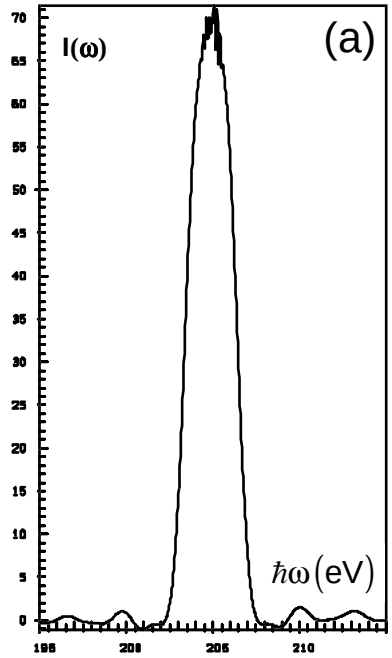

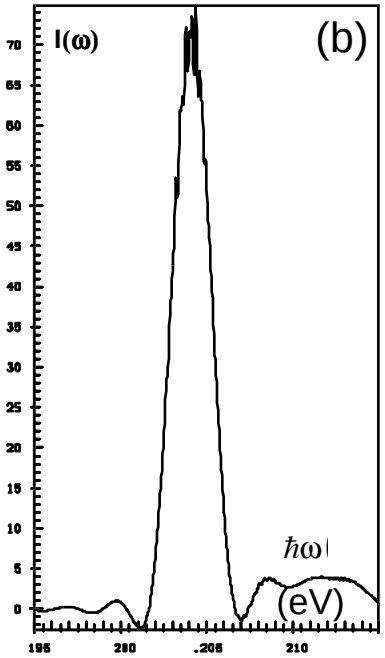

Figure 8 (continued next page).

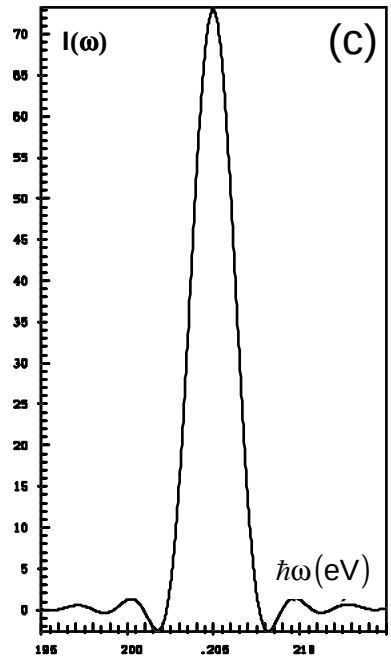

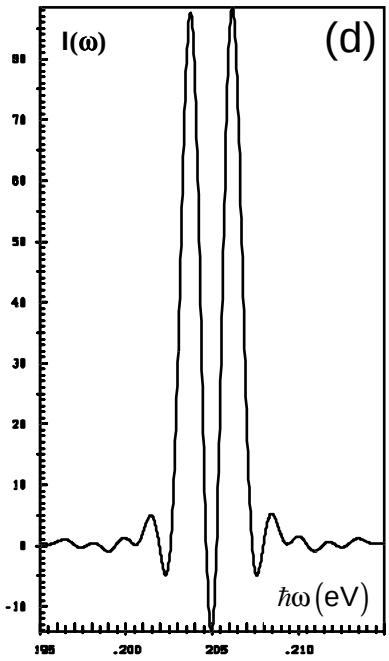

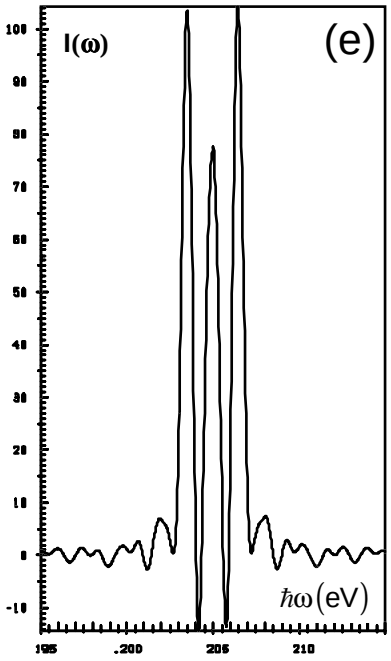

Figure 8 (continued). *Absorption cross sections I(ω) calculated from $|D_1>$ simulations at T = 0K (a, b) and 300 K (c, d, e) in arbitrary units [$I(\omega) = \sigma(\omega)/(8\pi^2\alpha a_0^2)$ is plotted, see text] as functions of the energy of the incident radiation ù for chains of 51 units (n_0 is the initial excitation site) and the following parameter values (4^{th} order Runge-Kutta method with 200000 time steps of a size of 0.15 fs; x = $1\cdot10^{-8}$).*
(a) W = 13 N/m, χ = 20 pN, n_0 = 1
(b) W = 13 N/m, χ = 60 pN, n_0 = 1
(c) W = 30 N/m, χ = 20 pN, n_0 = 1
(d) W = 30 N/m, χ = 20 pN, n_0 = 2
(e) W = 30 N/m, χ = 20 pN, n_0 = 3

behaviour occurs when the inital excitation is placed at the other end of the chain, namely the farther the initial excitation site is away from the respective chain end, the more bands show up. This feature is due to the fact, that the initial excitations probe different combinations of normal modes of the amide-I chain. One could think that this feature might be an experimental probe for the existence of Davydov solitons in proteins. Already in Figure 8c the peak is much smaller than the normal amide-I band as measured with conventional vibrational spectroscopy. This broadening in the latter case might probably be due to couplings which are not present in our model. However, a further difficulty is, that such splittings and the corresponding solitary waves can only be obtained from localized initial excitations, while the irradiation for the determination of spectra usually excites just normal modes, which are delocalized. However, to get a clear insight, let us investigate such initial excitations more in detail. Namely, the Hamiltonian of the decoupled amide-I system

$$\hat{H}_e = -J\sum_n \left(\hat{a}_n^+\hat{a}_{n+1} + \hat{a}_{n+1}^+\hat{a}_n\right) = -J\,\underline{\hat{a}}^+\,\underline{\underline{X}}\,\underline{\hat{a}}$$

$$X_{nm} = \delta_{m,n+1}(1-\delta_{nN}) + \delta_{m,n-1}(1-\delta_{n1}) \qquad (48)$$

can be brought into diagonal form via

$$\underline{\underline{W}}^{+}\,\underline{\underline{X}}\,\underline{\underline{W}} = \underline{\underline{\varepsilon}}\,; \quad \varepsilon_{k'k} = \varepsilon_k \delta_{k'k}$$

$$\hat{H}_e = -J \sum_k \varepsilon_k \hat{d}_k^{+}\ \hat{d}_k\ ; \quad \underline{\hat{d}} = \underline{\underline{W}}^{+}\underline{\hat{a}} \tag{49}$$

Then we can write our initial excitation (at site n_0) in the form

$$|\varphi(0)> = \sum_n a_n(0)\hat{a}_n^{+}|0> = \sum_k d_k(0)\hat{d}_k^{+}|0>$$
$$a_n(0) = \delta_{n,n_0} \quad ; \quad d_k(0) = \sum_n W_{nk}^{*} a_n(0) = W_{n_0,k}^{*} \tag{50}$$

Therefore we can compute the initial occupation of the normal modes, $|d_k(0)|^2$, for different initial excitation sites n_0. The results are shown in Table 1 (note, that in the course of the simulation, these modes become coupled via the nonlinearity). From the Table it is obvious, that for $n_0 = 1$ we probe just one set of normal modes around the centre of the band, resulting in one line in the spectrum. For $n_0 = 2$ we already excite two sets of normal modes around the centre of the complete amide-I band, which itself has no intensity. Thus we obtain a splitting into two bands. For $n_0 = 3$ we already have three sets of normal modes initially occupied, leading to three lines in the spectrum, and so forth.

In case of a complete dispersion, i.e. ideally with a vanishing nonlinearity and periodic boundary conditions such a splitting of bands does not occur. This is most easily seen, if we insert the exact wave function [eq. (C12) in [14]] of a decoupled oscillator system with one-site initial excitation, together with its phase factor (periodic boundary conditions), into equation (35) and (34) for the absorption cross section. The zero point energy of the lattice cancels out, and the cross section is

$$\sigma(\omega) = \frac{8\pi^2 \alpha a_0^2 \omega}{N} \sum_k \mathrm{Re}\left[\int_0^{\infty} e^{i(\omega-\bar{\omega}_k)t}\,dt\right] =$$
$$= \frac{4\pi^2 \alpha a_0^2 \omega}{N} \sum_k \int_{-\infty}^{\infty} e^{i(\omega-\bar{\omega}_k)t}\,dt = \frac{8\pi^3 \alpha a_0^2}{N}\,\omega \sum_k \delta(\omega - \bar{\omega}_k) \tag{51}$$
$$\bar{\omega}_k = \frac{1}{\hbar}\left[\varepsilon_0 - 2J\cos\left(\frac{2\pi}{N}k\right)\right]$$

(for cyclic boundary conditions). Thus the spectrum of a freely dispersing one-site initial excitation would be just a very dense superposition of delta-function peaks and completely independent of the initial excitation site, as one has to expect for the case of periodic boundary conditions. However, for a finite open chain the situation is different.

As mentioned already, it is difficult to excite just one site in a chain by a laser pulse. Thus we want next to examine the dynamics of an initially excited normal mode of the dipole-coupled system of free oscillators and the resulting spectra. In Figure 9 a-d the dynamics resulting from an initial excitation of the normal mode no. 5 (numbered in increasing order of eigenvalues) of the free amide-I oscillator system at T = 0 K and T = 300 K are shown. Obviously, the different peaks in

Table 1. *Normal mode (of the amide-I oscillator system with dipole coupling only) occupancies $|d_k(t = 0)|^2$ for a chain of 51 units (J = 0.967 meV) for different wave numbers k of the amide-I system (dipole coupling only) and different initial excitation sites n_0 (all other sites are unexcited in the respective initial states). Note that due to symmetry $|d_{26-k}(t = 0)|^2 = |d_{26+k}(t = 0)|^2$ holds.*

k	n_0=1	n_0=2	n_0=3
1	0.0001	0.0006	0.0012
2	0.0006	0.0022	0.0048
3	0.0012	0.0048	0.0103
4	0.0022	0.0083	0.0169
5	0.0034	0.0124	0.0238
6	0.0048	0.0169	0.0302
7	0.0065	0.0215	0.0351
8	0.0083	0.0261	0.0379
9	0.0103	0.0302	0.0383
10	0.0124	0.0336	0.0363
11	0.0146	0.0363	0.0320
12	0.0169	0.0379	0.0261
13	0.0192	0.0385	0.0192
14	0.0215	0.0379	0.0124
15	0.0238	0.0363	0.0065
16	0.0261	0.0336	0.0022
17	0.0282	0.0302	0.0001
18	0.0302	0.0261	0.0006
19	0.0320	0.0215	0.0034
20	0.0336	0.0169	0.0083
21	0.0351	0.0124	0.0146
22	0.0363	0.0083	0.0215
23	0.0372	0.0048	0.0282
24	0.0379	0.0022	0.0336
25	0.0383	0.0006	0.0372
26	0.0385	0.0000	0.0385

the $|a_n|^2$ distribution of the normal mode become coupled to the lattice and break up into distinct pinned solitons, as the lattice displacements at T = 0 K show. At T = 300 K the same phenomenon occurs, however, due to thermal fluctuations the localization becomes enhanced (Anderson localization in addition to nonlinear localization) and consequently the number of pinned solitary waves formed equals now the number of maxima in the $|a_n|^2$ distribution of the mode. Figure 10 a,b display the spectra as calculated from these dynamics. The spectra show clearly, that not only the normal mode, which is excited initially, shows up (the line with the largest intensity) in the spectrum but it is mixed through the nonlinear coupling with other ones. At T = 300 K (Figure 10b), the normal mode structure of the spectrum is now superimposed on a broad quasi-continuum due to the lattice phonons. The solitons formed from the normal mode excitation do not result in special features in the spectra. In Fig 9 e-h the corresponding dynamics after an initial excitation of one of the higher normal modes (49) are displayed and in Figure 10 c,d the corresponding spectra. Due to the fact, that this normal mode has a large number of nodes, we observe formation of a solitary wave from a quasi-random background only after longer times. The spectra show more or less the same features as for the 5th mode. The conclusion from these calculations is, that also from initial normal mode excitations solitary waves can be formed and that they do not give rise to special features in the spectra. However, thermal broadening obviously is able to make any fine structures invisible. This is not obvious from our former single-site excitation spectra, because there a smaller number of phonons becomes active.

Finally, let us assume, that we have a sample containing completely regular alpha helical segments with identical amino acid residues. If such a sample could be synthesized at all, one could also think about a measurement of initial one-site excitations by irradiation with a monochromatic laser pulse at 0.205 eV (1653.56 cm^{-1}). Assume that we could irradiate within a short, well defined time, which would lead to a broadening of the pulse in frequency space according to the time the pulse lasts, as given by the Fourier analysis of such a pulse. Let us look at such an irradiation with the time dependent electric field (α being real)

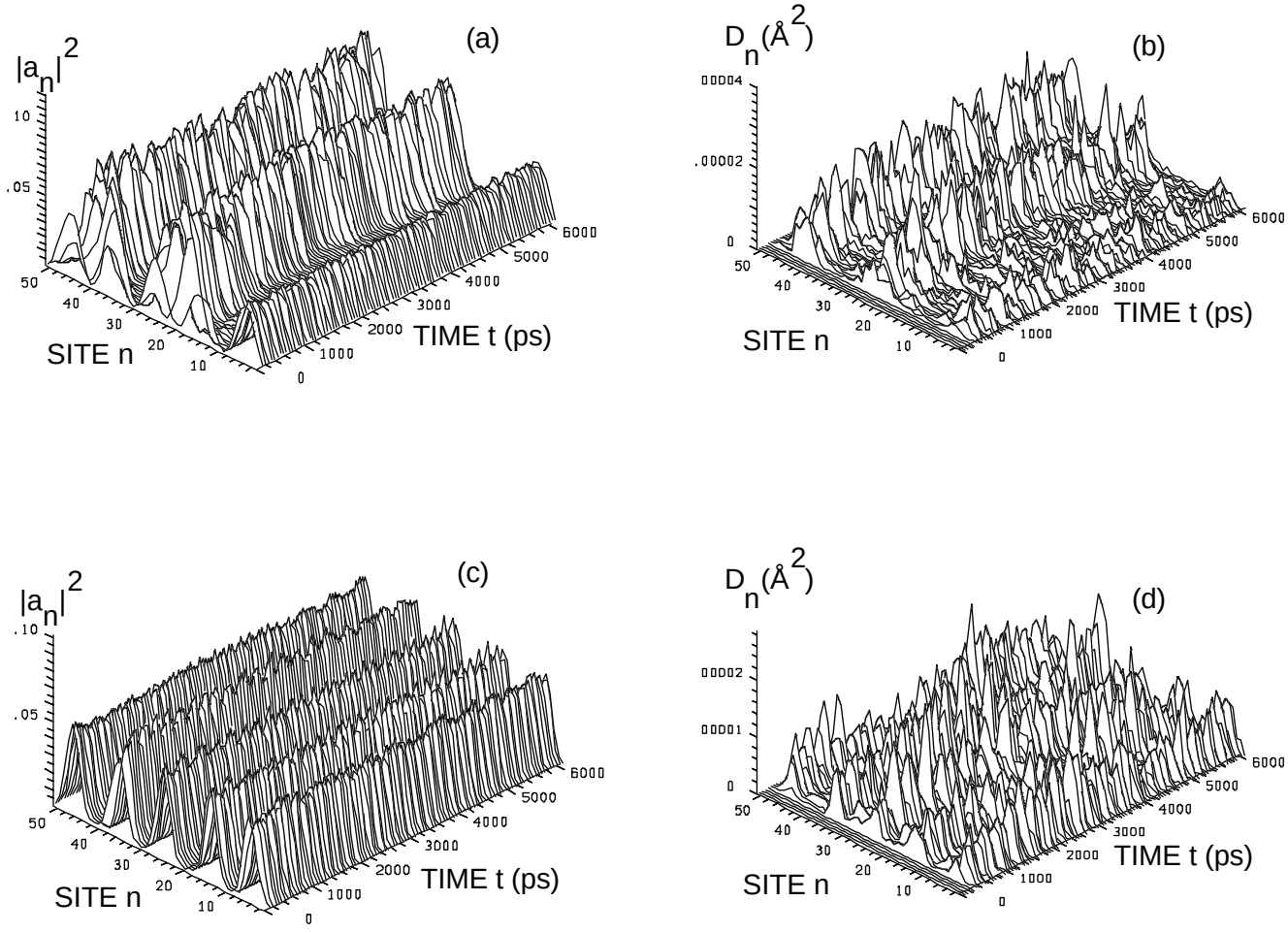

Figure 9 (continuous next page).

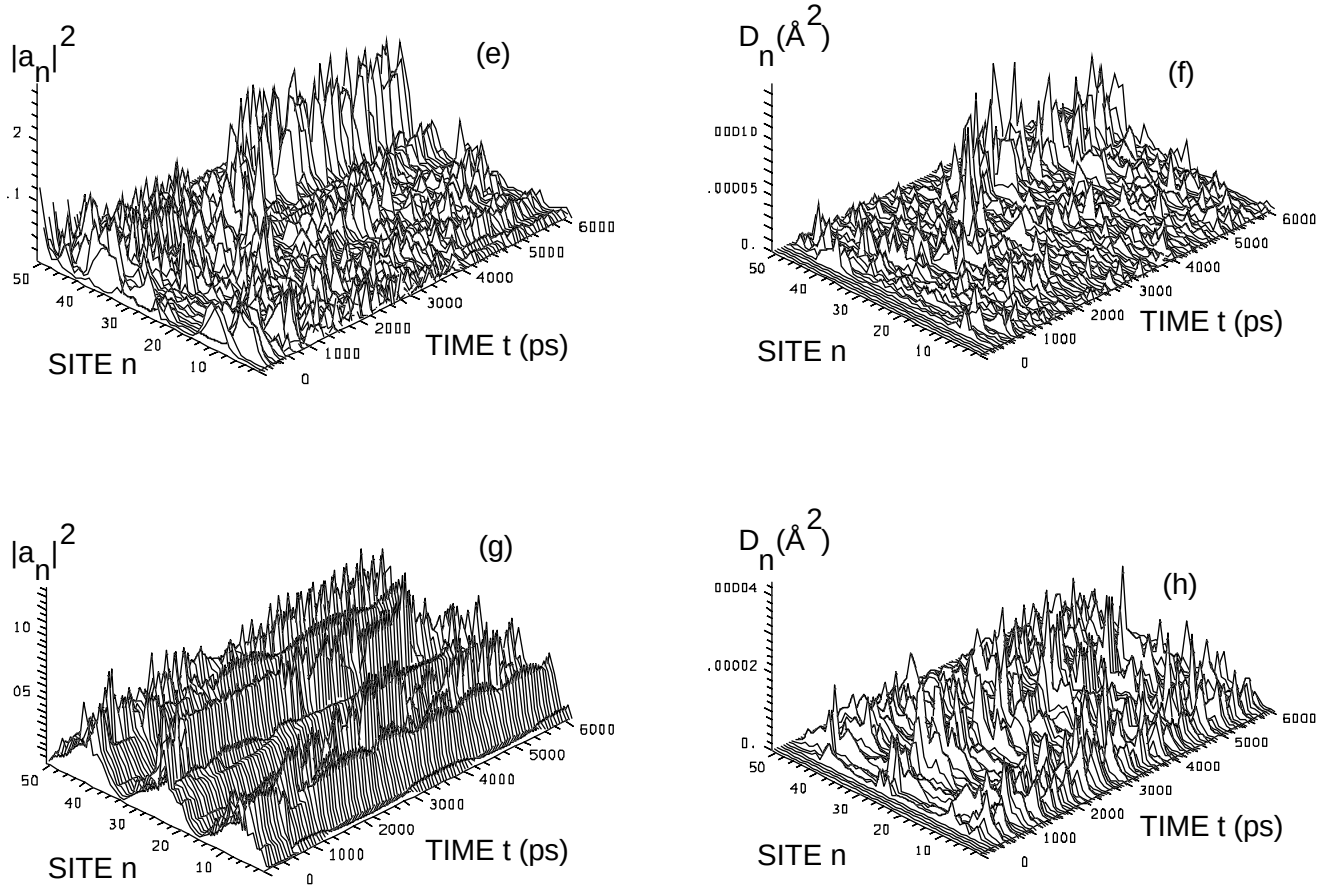

Figure 9. *The probability $|a_n|^2$ (a, c, e, g) and the squared local lattice deformation D_n (b, d, f, h) as functions of site n and time t for the time evolution of one amide-I quantum, initially excited in form of one normal mode k (numbering according to increasing energy) of the decoupled oscillator system for J = 0.967 meV, W = 13 N/m and χ = 60 pN for two values of k and different temperatures, T = 0 K and 300 K, in an open chain of 51 units, using the $|D_1>$ ansatz and the averaged Hamiltonian model (the time step size was 1.5 fs, the number of steps was 4,000,000 and a 4th order Runge-Kutta method was used; x = 1·10^{-8}).*
(a, b) K = 5, T = 0 K (c, d) K = 5, T = 300 K
(e, f) K = 49, T = 0 K (g, h) K = 49, T = 300 K

$$E(t) = E_0 \cdot \cos(\omega_0 t) \cdot e^{-\alpha r^2} = \\ = \frac{1}{2} E_0 \left(e^{i\omega_0 t} + e^{-i\omega_0 t} \right) \cdot e^{-\alpha r^2} \tag{52}$$

Then its Fourier transformation can be rewritten, using Euler's formula, and considering even (sine) and odd (cosine) functions (with respect to time) in the integrands, to a sum of two Fourier cosine- transformations of the Gaussian (ω_0 denotes the frequency of the incident monochromatic pulse):

$$\overline{E}(\omega) = \frac{1}{2} E_0 \int_{-\infty}^{\infty} \left(e^{i\omega_0 t} + e^{-i\omega_0 t} \right) \cdot e^{-\alpha r^2} e^{-i\omega t} dt = \\ = E_0 \left[\int_0^{\infty} \cos(\omega_1 t) e^{-\alpha r^2} dt + \int_0^{\infty} \cos(\omega_2 t) e^{-\alpha r^2} dt \right] = \\ \left(\omega_{1,2} = \omega_0 \pm \omega \right) = \frac{1}{2} \sqrt{\frac{\pi}{\alpha}} E_0 \left[e^{-\frac{(\omega_0 + \omega)^2}{4\alpha}} + e^{-\frac{(\omega_0 - \omega)^2}{4\alpha}} \right] \tag{53}$$

With the help of this well-known relation it might be possible to create a pulse, with a frequency distribution which is close in form to that one for a one-site excitation as given in Table 1. To simulate such a situation, we created a Gaussian packet of normal modes around its center $k_0 = 26$ ($\omega_0 = 0.205$ eV):

$$|d_k(t=0)|^2 = a f_k \quad ; \quad f_k = e^{-\frac{(\omega_0 - \omega_k)^2}{4\alpha}} + e^{-\frac{(\omega_0 + \omega_k)^2}{4\alpha}}$$

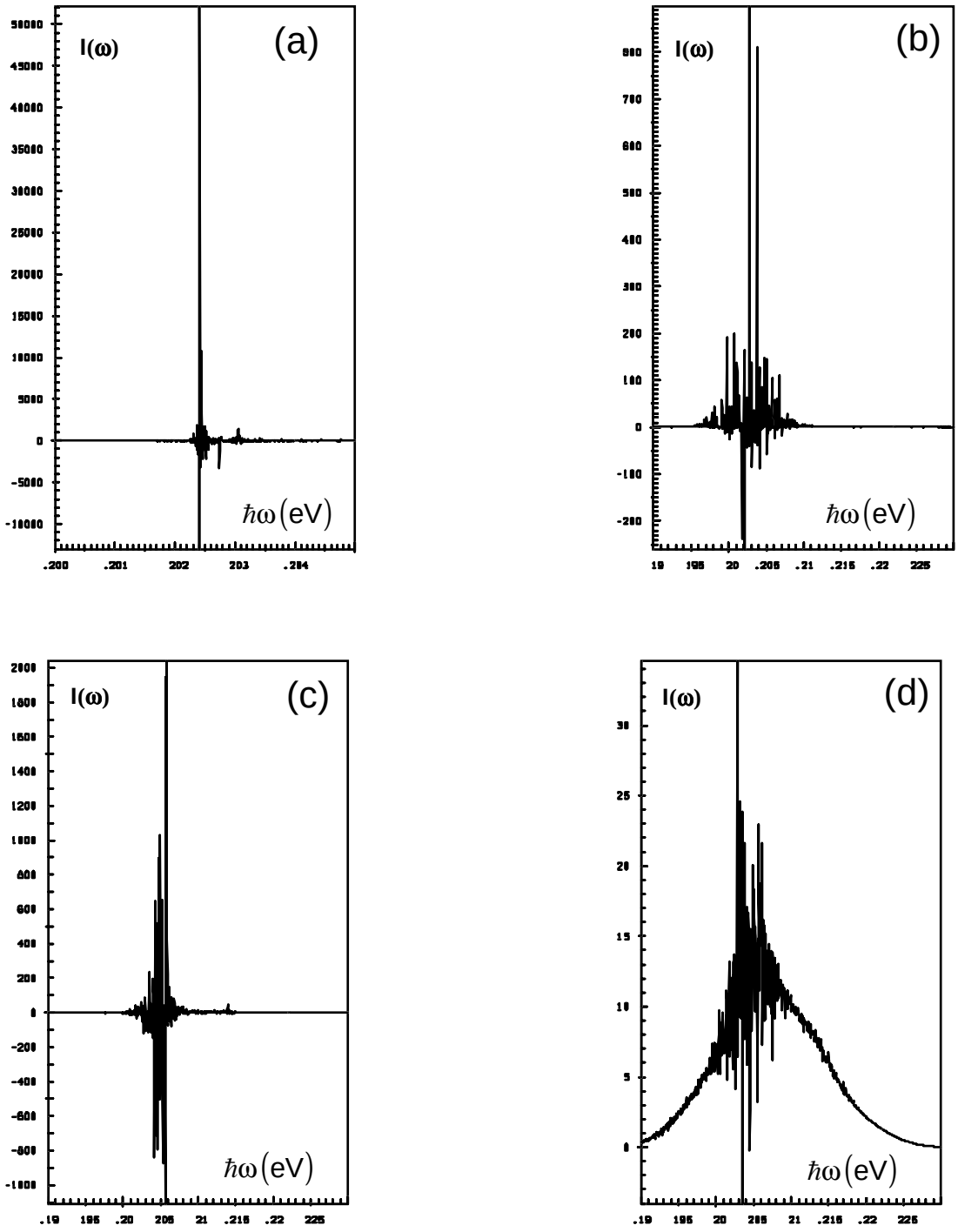

Figure 10. *Absorption cross sections I(ω) calculated from the $|D_1>$ simulations shown in Figure 9 in arbitrary units [$I(\omega) = \sigma(\omega)/(8\pi^2\alpha a_0^2)$ is plotted, see text] as functions of the energy of the incident radiation ù for chains of 51 units (k is the initially excited normal mode of the decoupled oscillator system; 4th order Runge-Kutta method with 4,000,000 time steps of a size of 1.5 fs; x = $1\cdot10^{-8}$). Note, that the artificial negative peaks in the spectra are here somewhat larger than in Fig. 8, because we use a larger step size in the numerical time integration (Simpson method) than there.*

(a) K = 5, T = 0 K *(b) K = 5, T = 300 K*
(c) K = 49, T = 0 K *(d) K = 49, T = 300 K*

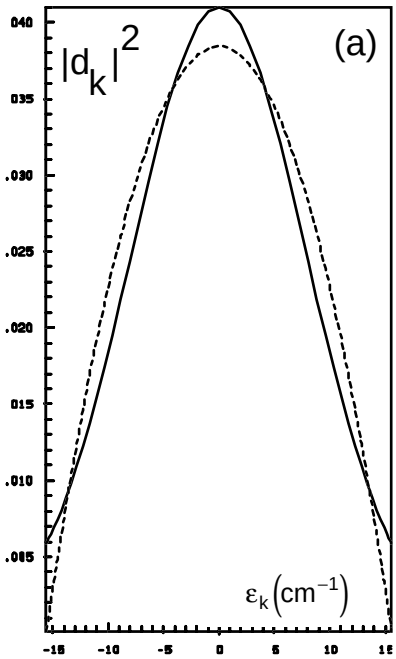

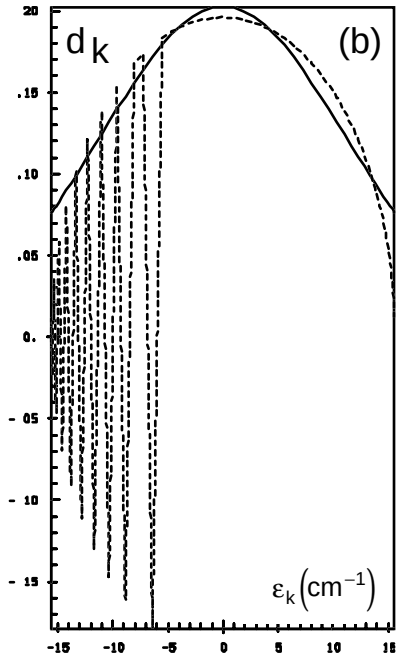

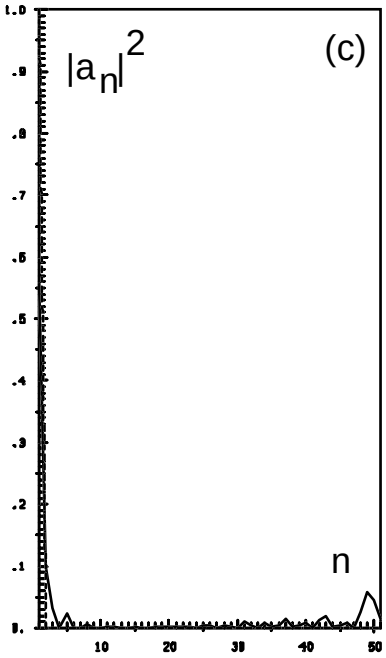

Figure 11. *Comparison between a Gaussian packet (solid lines) of normal modes from eq. (54) and the correct distribution for initial excitation $n_0 = 1$ from eq. (50) (Table 1, dashed lines) as functions of the eigenenergies ε_k of the normal modes of the decoupled oscillator system relative to 0.205 eV (open chain, 51 units, J = 0.967 meV):*

(a) $|d_k(t = 0)|^2$.

(b) $d_k(t = 0) = |d_k(t = 0)|$ *(in case of the Gaussian packet only the square root of (a) can be taken; solid line) and* $d_k(t = 0) = W^*_{1,k}$ *according to eq. (50) (dashed line).*

(c) $|a_n(t = 0)|^2$ *as resulting from the two distributions given in (b).*

$$a = \frac{1}{\sum_k f_k} \quad ; \quad \Delta = \sum_k \left[|W^*_{1,k}|^2 - a f_k \right]^2 = \min \tag{54}$$

$$\Rightarrow \alpha = 1.103\,\mathrm{ps}^{-2} \quad \text{with} \quad \Delta_{\min} = 0.525 \cdot 10^{-3}$$

This normalized distribution results in an approximate initial excitation at site 1. In Figure 11 we show a comparison between the Gaussian pulse and the one from Table 1 for $n_0 = 1$. It is obvious, that the squares are very similar in both cases. However, from the Gaussian pulse we can only obtain the simple square roots to get the $d_k(t = 0)$, and thus we do not reproduce the oscillatory feature on the low energy side of the exact distribution, which leads to an initial excitation which is localized mainly at site n = 1, but has in addition some small contributions at other sites also. The width of such a Gaussian pulse (with a monochromatic irradiation at 0.205 eV), representing approximately an initial excitation at site $n_0 = 1$, in frequency space corresponds roughly to (from Table 1) 11.03 cm^{-1}, and thus to an irradiation time (about 0.95 ps) which can be computed from the Fourier analysis of the form of the pulse as a function of time. The width can be estimated via ($\Delta k = 13$ here)

$$\Delta\omega = \frac{1}{\hbar}|\varepsilon_{k_0} - \varepsilon_{k_0-\Delta k}| \quad ; \quad \underline{\underline{X}}^{+}\,\underline{\underline{J}}\,\underline{\underline{X}} = \underline{\underline{\varepsilon}}$$
$$\varepsilon_{k'k} = \varepsilon_k \delta_{k'k} \qquad (55)$$
$$J_{n'n} = -J\left[\delta_{n',n+1}\left(1-\delta_{nN}\right) + \delta_{n',n-1}\left(1-\delta_{n1}\right)\right]$$

If such an experiment could be done at all nowadays is very questionable, because of (a) the well defined samples necessary, (b) the also well defined irradiation to excite initially a defined packet of normal modes, within a small energy spacing of about ±2 meV around ε_0 = 0.205 eV and (c) the resolution which is necessary to measure e.g. distinct absorbtion peaks of such small widths and seperations, to be able to distinguish between a soliton signal and the conventional amide-I band. Furthermore, such a hypothetical experiment would have to be carried out at a temperature as low as possible, to avoid any kind of thermal broadening of spectral lines on one hand, and to exclude a thermal excitation of other vibrations in the system, not included in the model, which might couple to amide-I on the other hand. Further the intensity of the irradiation should be small enough that only one-photon absorptions occur.

As we have discussed above, the initial excitation which could be obtained from a laser pulse (see Figure 11) does not represent a clean one-site excitation. On the contrary about 40% of the excitation would be distributed onto other sites also. Thus we performed simulations with exactly the initial excitation from Figure 11 at different temperatures and calculated the corresponding spectra. Figure 12 shows the time evolution of such a Gaussian packet of normal modes as initial excitation and Figure 13 the corresponding spectra. Obviously, the deviations from a one-site excitation at n_0 = 1, which would be unavoidable in a real experimental setting, lead to dynamics which are considerably different from those obtained from a clean one-site excitation.

From Figure 12a and b it is obvious, that from the initial excitation a solitary is formed at 0 K, which is able to travel several times through the chain, followed by its stabilizing lattice distortion (b). From the excitation at the other chain end, a dispersing wave train is formed. The spectrum (Figure 13a) shows clearly, that all the normal modes of the chain

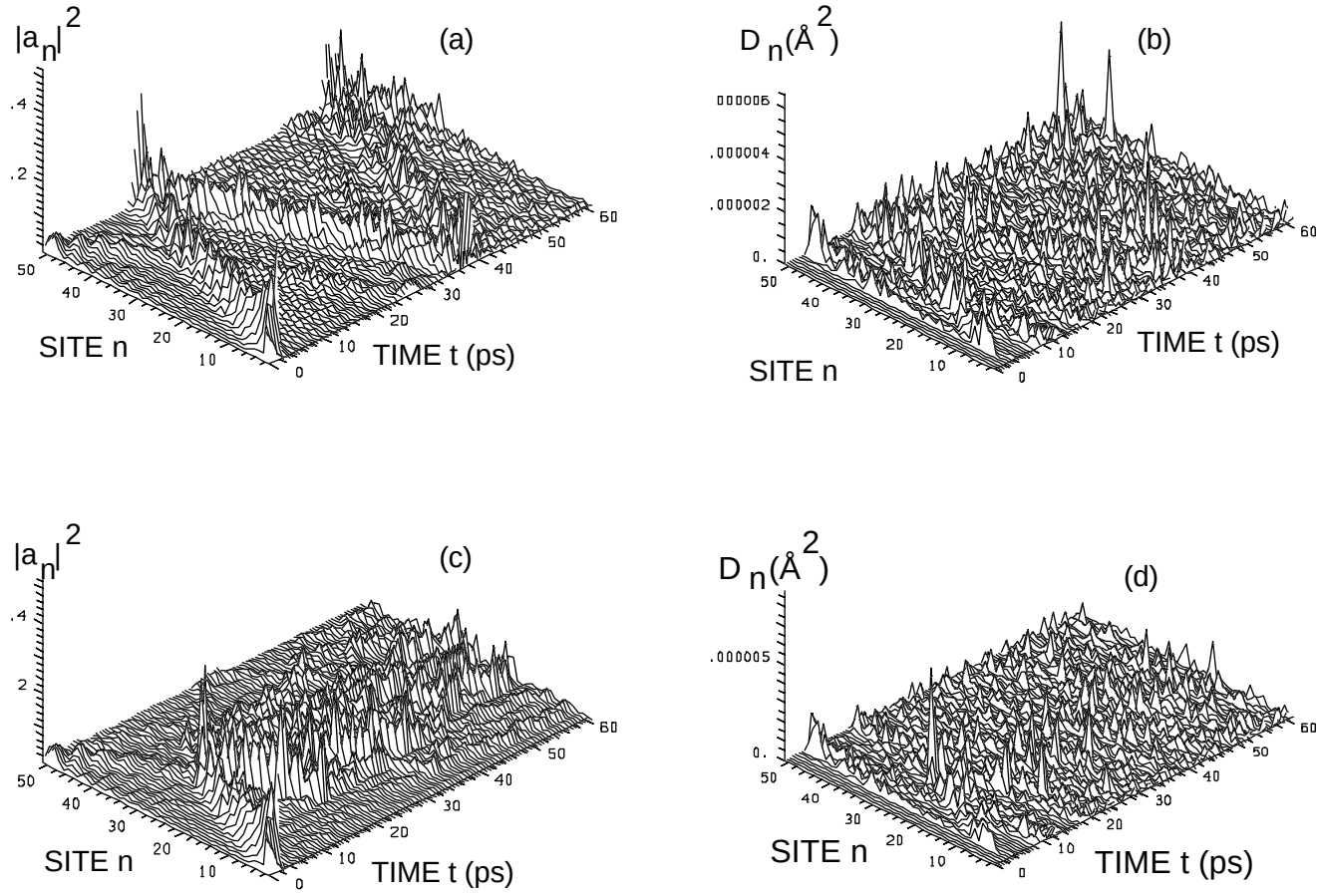

Figure 12 (continued next page).

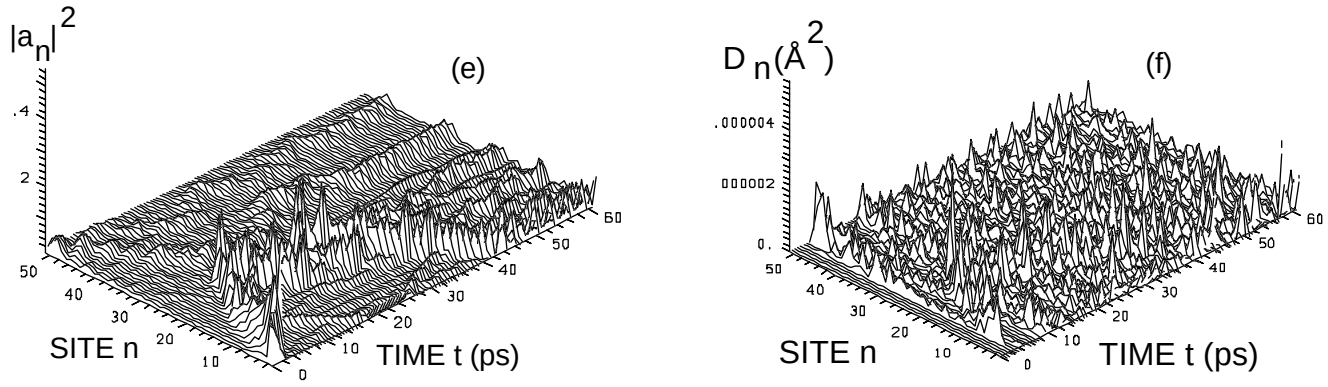

Figure 12. *The probability $|a_n|^2$ (a, c, e) and the squared local lattice deformation D_n (b, d, f) as functions of site n and time t for the time evolution of the Gaussian packet of normal modes shown in Figure 11 for J = 0.967 meV, W = 30 N/m and χ = 20 pN for three different temperatures, T = 0 K, 150 K and 300 K, in an open chain of 51 units, using the $|D_1>$ ansatz and the averaged Hamiltonian model (with 400,000 time steps of a size of 0.15 fs and a 4th order Runge-Kutta method; $x=1\cdot10^{-8}$).*
(a,b) T = 0 K (c, d) T = 150 K (e, f) T = 300 K

become excited via the nonlinear coupling and give a signal in the band, which is much more complicated than the spectra of the clean one-site excitations (Figure 8). At 150 K (Figure 12 c,d) the solitary wave started from site 1 is repelled when it hits the wave train coming from the other chain end in the middle of the chain. After some oscillation the two features merge to a very broad, localized and pinned excitation. This behaviour gives rise to an asymmetry of the band in the spectrum (Figure 13b), which is now more dense on its lower energy side. Finally, at 300 K (Figure 12 e,f), the initially formed solitary wave again becomes repelled by the wave train from the other side of the chain. However, it seems that at roughly 30 ps the two features merge to a solitary wave, traveling just once to the chain end. Afterwards the exciation breaks up in several distinct, localized and pinned features of very small amplitude. The absorption band (Figure 13c) seems now to be somewhat smaller, but still has a complicated structure, however, a very simple overall shape, which anyway is what could be measured. Thus it seems that it is impossible to obtain one-site excitations from laser pulses, which are clean enough to give the regular spectral features which we discussed above. Moreover, the strong dependence of the results on the initial excitation suggests that we deal here with a system showing chaotic behaviour, as most nonlinear systems do. This possibility will be the subject of future studies.

To obtain a clearcut distinction, whether or not solitons are formed one could also think of a situation where a splitting of the amide-I band into two or three very close peaks occurs. For this case one would need the excitation e.g. of two close-by frequencies with a well defined packet of normal modes around them. The time, the two lasers would have to irradiate the chain in order to create a one-site excitation at its second site could be determined again from the Fourier analysis of a pulse with defined frequency, lasting for a finite time, such that each of the two pulses creates one of the two normal mode distributions as given e.g. in Table 1 for $n_o = 2$. The chain lengths would have to be large enough, that the normal mode distribution for the creation of an excitation at a terminal site is not much influenced by small variations of the chain lengths in the sample. However, in our case the frequencies of the two lasers would have to be 1642.53 cm^{-1} and 1664.59 cm^{-1}, and the widths in frequency space have to be roughly 3.195 cm^{-1}. The problem is, that as discussed above laser pulses are not able to give a one-site excitation clean enough to produce the features discussed in the spectra. Therefore, such a possibility for soliton detection most probably is not a realistic one. In Appendix B we discuss one-site excitatons in open chains without nonlinearity, to be sure, whether or not the band splittings occurring in the spectra (Figure 8) are a trace of soliton formation. Indeed, band splittings also occur in the spectra formed from free dispersion in the open chain.

Conclusions

As next steps in our investigations we want to perform computations of this kind with a $|D_1>$ like model for acetanilide (ACN) where the spectra of the amide-I vibration are available in a wide range of temperatures [42]. Thus calculations of this kind can be used for a direct check of theoretical models against experiment. In ACN Frank-Condon factors are larger than in proteins, because in the former case the C=O oscillators are coupled to optical phonons, rather than to acoustical ones as in proteins. Further we apply in the moment our $|D_1>$ equations for more than one quantum of amide-I vibration to see, whether also in the $|D_1>$ case solitons become more stable when the number of quanta they carry increases or not.

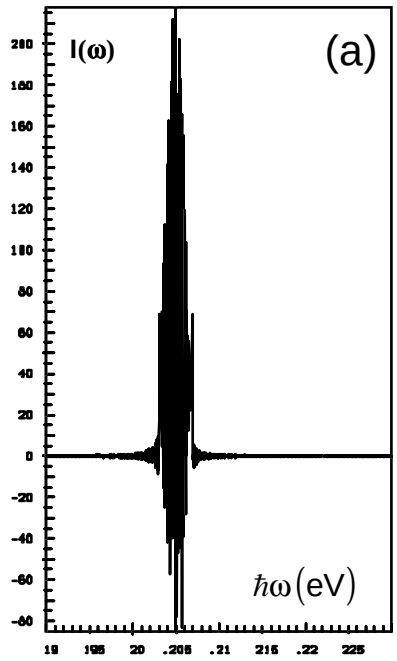

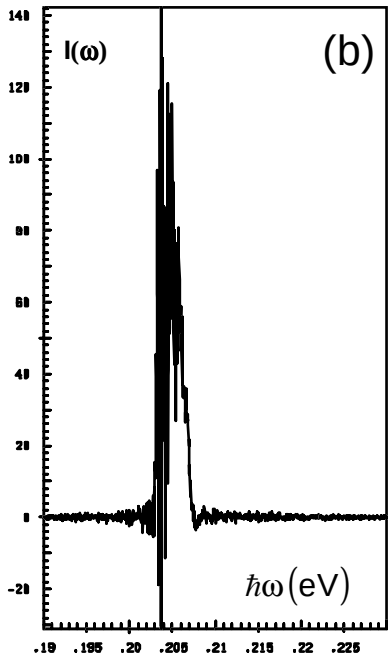

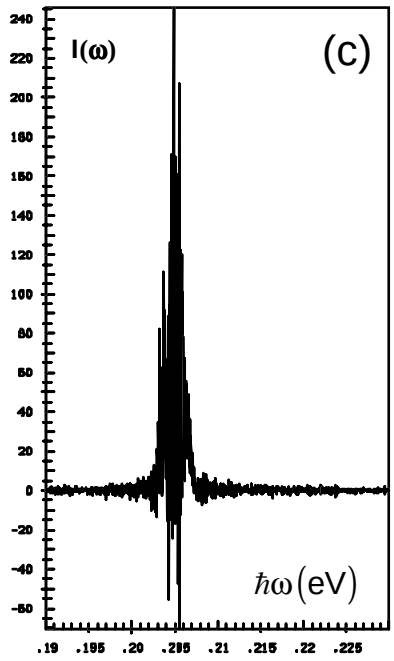

Figure 13. *Absorption cross sections I(ω) calculated from the $|D_1>$ simulations shown in Figure 12 in arbitrary units [$I(\omega) = \sigma(\omega)/(8\delta^2\alpha a_0^2)$ is plotted, see text] as functions of the energy of the incident radiation $\hbar\omega$ for chains of 51 units (4^{th} order Runge-Kutta method with 400,000 time steps of a size of 0.15 fs; $x = 1 \cdot 10^{-8}$).*
(a) T = 0 K (b) T = 150 K (c) T = 300 K

As Barthes [42] points out, it is of importance, to couple not only the amide-I vibration to the lattice phonons, but also vibrations which are of N-H type, because in the region of N-H vibrations the spectra of proteins show anomalous features (thus in this case one would need probably coupling of the amide-II vibration to optical phonons). Our basic conclusion from the above discussed results is first of all, that with the $|D_1>$ ansatz we have a state at hand with which we are able to describe the dynamics of the Davydov model with a high accuracy, at least at 0 K. Further, our comparisons with QMC results indicate that also the average Hamiltonian method of Davydov for the inclusion of temperature effects into the model yields at least qualitatively correct results. We could show, that within this model at 300 K Davydov solitons can be formed at reasonable values of the parameters, however, in contrast to the T = 0 K case, not only from initial states where the amide-I excitation is localized at the chain end with a C=O group involved in the coupling to the lattice, but also for initial excitations at the other chain end. Only from excitations inside the chain solitons cannot be formed. Whether this criterion is fulfilled in native proteins is still an open question. Earlier discussions indicate, that at least for actine [45] the ATP binding site is not directly attached to a helical segment, but to a random coil structured sequence of the protein. The energy released, could be stored in Anderson localized vibrational amide-I states due to the aperiodicity of a random coil region. Because of the disorder, dispersion would not occur probably. Then by a hopping mechanism, the energy packet could move as a whole between states which are localized on different sites, until it is finally injected into an α–helical segment. Thus it seems that it might well be possible, that the injection of the energy released by ATP hydrolysis into an α–helix occurs at well

defined terminal sites of the segment. However, one needs more structural details of the structure of such proteins to decide, whether this is the case. Finally, our investigations suggest a chaotic behaviour of the Davydov model system, which will be subject of future work.

Acknowledgement. The financial support of the „Deutsche Forschungsgemeinschaft“ (project-no. Fo 175/3-1) and of the „Fonds der Chemischen Industrie“ is gratefully acknowledged. Some parts of this work were presented on the 2nd International Congress of the International Society for Theoretical Chemical Physic in New Orleans, USA, on April 9-13, 1996.

References

1. Scott, A.C. *Phys. Rep.* **1992**, *217*, 1.
2. Davydov, A.S.; Kislukha, N.I. *Phys. Stat. Sol.* **1973**, *B59*, 465; Davydov, A.S. *Phys. Scripta* **1979**, *20*, 387.
3. Davydov, A.S. *Zh. Eksp. Teor. Fiz.* **1980**, *78*, 789; *Sov. Phys. JETP* **1980**, *51*, 397.
4. Scott, A.C. *Phys. Rev.* **1982**, *A26*, 57; *Physica Scripta* **1984**, *29*, 279; Mac Neil, L.; Scott, A.C. *Physica Scripta* **1984**, *29*, 284; *Phil. Trans. Roy Soc. London* **1985**, *A315*, 423.
5. Förner, W.; Ladik, J. In *Davydov's Soliton Revisited*; Christiansen, P.L.; Scott, A.C., Eds.; NATO ASI, Series B -Physics, Plenum New York, 1991, Vol. 243; p 267.
6. Förner, W. *J. Phys.: Cond. Matter* **1993**, *5*, 803.
7. Halding, J.; Lomdahl, P.S. *Phys. Lett.* **1987**, *A124*, 37.
8. (a) Lomdahl, P.S.; Kerr, W.C. *Phys. Rev. Lett.* **1985**, *55*, 1235; and in *Davydov's Soliton Revisited*, Christiansen, P.L.; Scott, A.C., Eds.; NATO ASI, Series B - Physics, Plenum, New York, 1991, Vol. 243; p 259. (b) Kerr, W.C.; Lomdahl, P.S. *Phys. Rev.* **1987**, *B35*, 3629. (c) Kerr, W.C.; Lomdahl, P.S. In *Davydov's Soliton Revisited*; Christiansen, P.L.; Scott, A.C., Eds.; NATO ASI, Series B - Physics, Plenum, New York, 1991, Vol. 243; p 23.
9. Lawrence, A.F.; McDaniel, J.C.; Chang, D.B.; Pierce, B.M.; Birge, R.R. *Phys. Rev.* **1986**, *A33*, 1188.
10. Bolterauer, H. In *Structure Coherence and Chaos in Dynamical Systems*; Christiansen, P.L.; Parmentier, R.D., Eds.; Proc. MIDIT **1986** Workshop, Manchester Univ. Press, England; Bolterauer, H. In *Davydov's Soliton Revisited*; Christiansen, P.L.; Scott, A.C., Eds.; Series B-Physics, Plenum, New YYork, 1991, Vol. 243; pp 99, 309.
11. Cottingham, J.P.; Schweitzer, J.W. *Phys. Rev. Lett.* **1989**, *62*, 1792; Schweitzer, J.W.; Cottingham, J.P. In *Davydov's Soliton Revisited*; Christiansen, P.L.; Scott, A.C., Eds.; NATO ASI, Series B - Physics, Plenum, New York, 1991, Vol. 243; p 285.
12. Motschmann, H.; Förner, W.; Ladik, J. *J. Phys.: Cond. Matter* **1989**, *1*, 5083.
13. (a) Förner, W. *J. Phys.: Cond. Matter* **1991**, *3*, 4333. (b) Förner, W. *J. Comput. Chem.* **1992**, *13*, 275.
14. Förner, W. *J. Mol. Model.* **1996**, *2*, 70.
15. Förner, W. *J. Mol. Model.* **1996**, *2*, 135.
16. Brown, D.W.; Linderberg, K.; West, B.J. *Phys. Rev.* **1986**, *A33*, 4104, 4110; *Phys. Rev.* **1987**, *B35*, 6169; *Phys. Rev.* **1988**, *B37*, 2946; Brown, D.W. *Phys. Rev.* **1988**, *A37*, 5010.
17. Cruzeiro, L.; Halding, J.; Christiansen, P.L.; Skovgaard, O.; Scott, A.C. *Phys. Rev.* **1988**, *A37*, 880.
18. Mechtly, B.; Shaw, P.B. *Phys.Rev.* **1988**, *B38*, 3075.
19. Skrinjar, M.J.; Kapor, D.V.; Stojanovic, S.D. *Phys. Rev.* **1988**, *A38*, 6402.
20. Förner, W. *Phys. Rev.* **1991**, *A44*, 2694; *J. Mol. Struct. (Theochem)* **1993**, *282*, 223.
21. Förner, W. *Nanobiology* **1992**, *1*, 413.
22. Förner, W. *J. Phys.: Cond. Matter* **1992**, *4*, 1915.
23. Wang, X.; Brown, D.W.; Linderberg, K. *Phys. Rev. Lett.* **1989**, *62*, 1796.
24. Scott, A.C. Presented at the *Conference on Nonlinear Sciences: The Next Decade*; Los Alamos, National Laboratory, on May 21, **1990**.
25. Brown, D.W.; Ivic, Z. *Phys. Rev.* **1989**, *B40*, 9876.
26. Förner, W. to be submitted to *J. Phys.: Condensed Matter*.
27. Förner, W. *J. Phys.: Cond. Matter* **1993**, *5*, 823.
28. Förner, W. *J. Phys.: Cond. Matter* **1993**, *5*, 3883.
29. Förner, W. *J. Phys.: Cond. Matter* **1993**, *5*, 3897.
30. Förner, W. *Physica* **1993**, *D68*, 68.
31. Förner, W. *J. Phys.: Cond. Matter* **1994**, *6*, 9089.
32. Förner, W. *Phys. Rev.* **1996**, *B53*, 6291.
33. Cruzeiro-Hansson, L.; Christiansen, P.L.; Scott, A.C. In *Davydov's Soliton Revisited*; Christiansen, P.L.; Scott, A.C., Eds.; Series B - Physics, Plenum, New York, 1991, Vol. 243; p 325.
34. Kapor, D. Remark in *Davydov's Soliton Revisited*; Christiansen, P.L.; Scott, A.C., Eds.; Series B - Physics, Vol. *243*; Plenum, New York (**1991**), 29.
35. Cruzeiro-Hansson, L.; Okhonin, V.A.; Khlebopros, R.G.; Yassievich, I.N. *Nanobiology* **1992**, *1*, 395.
36. Cruzeiro-Hansson, L. *Phys. Rev. Lett.* **1994**, *73*, 2927.
37. Förner, W. *J. Mol. Struct. (Theochem)* **1996**, *362*, 101.
38. Förner, W. (to be published).
39. Pierce, B.M. (private communication).
40. Förner, W. *J. Phys.: Condensed Matter* **1994**, *6*, 9089.
41. Peyrard, M., Ed; *Nonlinear Excitations in Biomolecules*; Springer Publishing Company, Berlin-Heidelberg (**1995**).
42. Barthes, M. In *Nonlinear Excitations in Biomolecules*; Peyrard, M., Ed; Springer, Berlin-Heidelberg, 1995, p 209.
43. Heller, E.J. *J. Chem. Phys.* **1978**, *48*, 2067.

44. Knox, R.S.; Maiti, S.; Wu, P. In *Davydov's Soliton Revisited*; Christiansen, P.L.; Scott, A.C., Eds.; Series B - Physics, Plenum, New York, 1991, Vol. 243; p 401.

45. Laki, K.; Ladik, J. In *Electronic Structure of Polymers and Molecular Crystals*; Andre, J.-M.; Ladik, J., Eds.; Plenum, New York, London, 1974, p 681.

Appendix A: Derivation of Davydov's Averaged Hamiltonian Method

Cruzeiro et al. [15] have given parts of the derivations necessary for this method. However, their derivation contains the Hamlitonian method as it was used by Davydov [2-3]. Skrinjar et al. [19] have shown, that in this case the choice of canonically conjugated momenta is not unique (see main text) and the derivation therefore yields incorrect equations of motion. The correct equations were given by us previously [22], however, without details of the derivation. Thus we want to describe in this Appendix for the first time the main steps of this procedure. As mentioned in the main text, Davydov started from the following ansatz-state:

$$|D_1,\nu>=\sum_n a_n(t)\hat{a}_n^+|0>|\beta_n,\nu> \quad ; \quad |\beta_n,\nu>=\hat{U}_n(t)|\nu> \quad ; \quad |\nu>=\prod_k \frac{\left(\hat{b}_k^+\right)^{\nu_k}}{\sqrt{\nu_k!}}|0>_p \tag{A1}$$

where $|0>_e$ denotes the exciton and $|0>_p$ the phonon vacuum. Note that in the product over normal modes k the translational mode has to be excluded. The unitary displacement operator is given by

$$\hat{U}_n(t)=\exp\left[\sum_k\left(b_{nk}(t)\hat{b}_k^+-b_{nk}^*(t)\hat{b}_k\right)\right]=\exp\left[-\frac{1}{2}\sum_k|b_{nk}(t)|^2\right]\cdot\exp\left[\sum_k b_{nk}(t)\hat{b}_k^+\right]\cdot\exp\left[-\sum_k b_{nk}^*(t)\hat{b}_k\right] \tag{A2}$$

where the second equality follows from the first one with the help of the Hausdorff formula:

$$e^{\hat{A}+\hat{B}}=e^{-\frac{1}{2}c}e^{\hat{A}}e^{\hat{B}} \quad , \quad c=\left[\hat{A},\hat{B}\right] \tag{A3}$$

which holds in this form if the commutator c is any complex number, but not an operator. Thus we can write

$$\hat{U}_n=e^{\hat{T}_n} \quad ; \quad \hat{U}_n^+=e^{\hat{T}_n^+}=e^{-\hat{T}_n} \quad \Rightarrow \quad \hat{U}_n^+\hat{U}_n=e^{-\hat{T}_n}\cdot e^{\hat{T}_n}=e^{-\hat{T}_n+\hat{T}_n}=\hat{1} \tag{A4}$$

Thus we have

$$<\beta_n,\nu'|\beta_n,\nu>=<\nu'|\hat{U}_n^+(t)\hat{U}_n(t)|\nu>=<\nu'|\nu>=\delta_{\nu\nu'} \tag{A5}$$

as mentioned in the main text we know further

$$\begin{aligned}&\hat{b}_k|\beta_n,\nu>=b_{nk}|\beta_n,\nu>+\sqrt{\nu_k}\,|\beta_n,\nu-1_k>\\&|\beta_n,\nu-1_k>\equiv\hat{U}_n|\nu-\overline{1_k}>=\hat{U}_n\prod_{k'}|\nu_{k'}-\delta_{k'k}>\end{aligned} \tag{A6}$$

This equation can be most easily derived by Taylor expansion of the exponentials in the coherent displacement operator with the help of

$$\hat{b}_k\left(\hat{b}_{k'}^+\right)^\nu=\left(\hat{b}_{k'}^+\right)^\nu\hat{b}_k+\nu\left(\hat{b}_{k'}^+\right)^{\nu-1}\delta_{k'k} \tag{A7}$$

which is easily proven by complete induction. Since a phonon annihilation operator for a given wave number k commutes with any phonon operator for another wave number k', we can restrict our considerations to that term of the product over wave numbers in the coherent state with the same wave number as our annihilation operator:

$$\begin{aligned}\hat{b}_k\,|\beta_{nk},\nu> &= e^{-\frac{1}{2}|b_{nk}|^2}\left[\sum_{\nu=0}^{\infty}\frac{b_{nk}^{\nu}}{\nu!}\hat{b}_k\left(\hat{b}_k^{+}\right)^{\nu}\right]e^{-b_{nk}^{*}\hat{b}_k}\,|\nu_k> \\ &= e^{-\frac{1}{2}|b_{nk}|^2}\left[\sum_{\nu=0}^{\infty}\frac{b_{nk}^{\nu}}{\nu!}\left(\hat{b}_k^{+}\right)^{\nu}\hat{b}_k+\sum_{\nu=0}^{\infty}\frac{b_{nk}^{\nu}}{\nu!}\left(\hat{b}_k^{+}\right)^{\nu-1}\right]e^{-b_{nk}^{*}\hat{b}_k}\,|\nu>=\hat{U}_{nk}\hat{b}_k\,|\nu>+b_{nk}\hat{U}_{nk}\;\nu>\end{aligned} \tag{A8}$$

which leads directly to eq. (A6).

Now we are in the position to compute expectation values of the phonon operators using

$$\begin{aligned}&<\beta_n,\nu|\beta_n,\nu>=1 \\ &<\beta_n,\nu|\beta_n,\nu-1_k>=<\nu|\hat{U}_n^{+}(t)\hat{U}_n(t)|\nu-1_k>=<\nu|\nu-1_k> \\ &=\prod_{k'}<\nu_{k'}|\nu_{k'}-\delta_{k'k}>=<\nu_k|\nu_k-1>\prod_{k'\neq k}<\nu_{k'}|\nu_{k'}>=0\end{aligned} \tag{A9}$$

as

$$\begin{aligned}<\beta_n,\nu\,|\hat{b}_k\,|\beta_n,\nu> \;&=\; b_{nk}<\beta_n,\nu\,|\beta_n,\nu> \;+\; \sqrt{\nu_k}<\beta_n,\nu\,|\beta_n,\nu-1_k> \;=\; b_{nk} \\ <\beta_n,\nu\,|\hat{b}_k^{+}\,|\beta_n,\nu> \;&=\; b_{nk}^{*}\end{aligned} \tag{A10}$$

The second equality holds because a phonon creation operator acts on a bra-state like an annihilator on a ket-state. In the same way we obtain

$$\begin{aligned}<\beta_n,\nu\,|\hat{b}_k^{+}\hat{b}_k\,|\beta_n,\nu> \;&=\; |b_{nk}|^2<\beta_n,\nu\,|\beta_n,\nu>+b_{nk}^{*}\sqrt{\nu_k}<\beta_n,\nu\,|\beta_n,\nu-1_k>+ \\ &+b_{nk}\sqrt{\nu_k}<\beta_n,\nu-1_k\,|\beta_n,\nu>+\nu_k<\beta_n,\nu-1_k\,|\beta_n,\nu-1_k> \;=\; |b_{nk}|^2+\nu_k\end{aligned} \tag{A11}$$

As next step we need

$$\begin{aligned}&e^{b_{nk}\hat{b}_k^{+}}\hat{b}_k=\left(\hat{b}_k-b_{nk}\right)e^{b_{nk}\hat{b}_k^{+}} \\ &\Rightarrow e^{-\frac{1}{2}\sum_k|b_{nk}|^2}\cdot e^{\sum_k b_{nk}\hat{b}_k^{+}}\cdot\hat{b}_k e^{-\sum_k b_{nk}^{+}\hat{b}_k}\,|\nu>=\left(\hat{b}_k-b_{nk}\right)|\beta_n,\nu>= \\ &=b_{nk}\,|\beta_n,\nu>+\sqrt{\nu_k}\,|\beta_n,\nu-1_k>=\sqrt{\nu_k}\,|\beta_n,\nu-1_k>\end{aligned} \tag{A12}$$

Now we are in the position to compute the time derivative of a unitary displacement operator acting on an arbitrary distribution of phonons:

$$\frac{\partial}{\partial t}|\beta_n,\nu> = \frac{\partial}{\partial t}\left[e^{-\frac{1}{2}\sum_k |b_{nk}|^2} \cdot e^{\sum_k b_{nk}\hat{b}_k^+} \cdot e^{-\sum_k b_{nk}^*\hat{b}_k} \right]|\nu> = -\frac{1}{2}\sum_k \left(\dot{b}_{nk} b_{nk}^* + b_{nk}\dot{b}_{nk}^*\right)|\beta_n,\nu> +$$
$$+\sum_k \dot{b}_{nk}\hat{b}_k^+ |\beta_n,\nu> - \sum_{k'} \dot{b}_{nk'}^* \cdot e^{-\frac{1}{2}\sum_k |b_{nk}|^2} \cdot e^{\sum_k b_{nk}\hat{b}_k^+} \hat{b}_{k'} \cdot e^{-\sum_k b_{nk}^*\hat{b}_k} |\nu> = \tag{A13}$$
$$= \sum_k \left[-\frac{1}{2}\left(\dot{b}_{nk} b_{nk}^* + b_{nk}\dot{b}_{nk}^*\right) + \dot{b}_{nk}\hat{b}_k^+ \right]|\beta,\nu> - \sum_k \dot{b}_{nk}^* \sqrt{\nu_k}\, |\beta_n,\nu-1_k>$$

and the corresponding expectation value is therefore

$$<\beta_n,\nu|\frac{\partial^{\rightarrow}}{\partial t}|\beta_n,\nu> = -\frac{1}{2}\sum_k \left(\dot{b}_{nk} b_{nk}^+ + b_{nk}\dot{b}_{nk}^*\right)<\beta_n,\nu|\beta_n,\nu> +$$
$$+\sum_k \dot{b}_{nk} <\beta_n,\nu|\hat{b}_k^+|\beta_n,\nu> - \sum_k \dot{b}_{nk}^* \sqrt{\nu_k}\, <\beta_n,\nu|\beta_n,\nu-1_k> = \frac{1}{2}\sum_k \left(\dot{b}_{nk} b_{nk}^* - b_{nk}\dot{b}_{nk}^*\right) \tag{A14}$$

where the arrow at the time derivative indicates that it acts on the ket (an arrow in the other direction means action on the bra). From this follows

$$<\beta_n,\nu|\frac{\partial^{\leftarrow}}{\partial t}|\beta_n,\nu> = \left(<\beta_n,\nu|\frac{\partial^{\rightarrow}}{\partial t}|\beta_n,\nu>\right)^* = -\frac{1}{2}\sum_k \left(\dot{b}_{nk} b_{nk}^* - b_{nk}\dot{b}_{nk}^*\right) \tag{A15}$$

and with the definition

$$<\varphi|\frac{\partial^{\leftrightarrow}}{\partial t}|\varphi> \equiv <\varphi|\frac{\partial^{\rightarrow}}{\partial t}|\varphi> - <\varphi|\frac{\partial^{\leftarrow}}{\partial t}|\varphi> = <\varphi|\dot{\varphi}> - <\dot{\varphi}|\varphi> \tag{A16}$$

we can write

$$\frac{i\hbar}{2}<\beta_n,\nu|\frac{\partial^{\leftrightarrow}}{\partial t}|\beta_n,\nu> = \frac{i\hbar}{2}\sum_k \left(\dot{b}_{nk} b_{nk}^* - b_{nk}\dot{b}_{nk}^*\right) \tag{A17}$$

Now we can compute the Lagrangian for our ansatz state (A1):

$$L_\nu = L_\nu^t - H_\nu$$
$$L_\nu^t = \frac{i\hbar}{2}<D_1,\nu|\frac{\partial^{\leftrightarrow}}{\partial t}|D_1,\nu> \; ; \; H_\nu = <D_1,\nu|\hat{H}|D_1,\nu> \tag{A18}$$

using

$$_e<0|\hat{a}_m\hat{a}_n^+|0>_e = \delta_{mn}$$
$$D_{mn}(\nu) = <\beta_m,\nu|\beta_n,\nu> \; ; \; D_{nn}(\nu) = 1 \tag{A19}$$

we can calculate

$$< D_1, \nu | \frac{\partial^{\rightarrow}}{\partial t} | D_1, \nu > = < D_1, \nu | \sum_n \dot{a}_n \hat{a}_n^+ | 0 >_e | \beta_n, \nu > + < D_1, ny | \sum_n a_n \hat{a}_n^+ | 0 >_e \frac{\partial^{\rightarrow}}{\partial t} | \beta_n, \nu > =$$

$$= \sum_n \dot{a}_n a_n^* + \frac{1}{2} \sum_{nk} \left(\dot{b}_{nk} b_{nk}^* - b_{nk} \dot{b}_{nk}^* \right) | a_n |^2 \tag{A20}$$

and thus

$$L_\nu^t = \frac{i\hbar}{2} < D_1, \nu | \frac{\partial^{\leftrightarrow}}{\partial t} | D_1, \nu > = \frac{i\hbar}{2} \sum_n \left(\dot{a}_n a_n^* - a_n \dot{a}_n^* \right) + \frac{i\hbar}{2} \sum_{nk} \left(\dot{b}_{nk} b_{nk}^* - b_{nk} \dot{b}_{nk}^* \right) | a_n |^2 \tag{A21}$$

Davydov's idea is now, to form a thermal average

$$\begin{aligned} L(T) &= L^t(T) - H(T) = \sum_\nu \rho_\nu(T) L_\nu^t - \sum_\nu \rho_\nu(T) H_\nu \\ \rho_\nu(T) &= \frac{f_\nu(T)}{\sum_\mu f_\mu(T)} \quad ; \quad f_\nu(T) = < \nu | \exp\left[-\frac{\hat{H}_p}{k_B T} \right] | \nu > \\ \hat{H}_p &= \sum_k \hbar\omega_k \left(\hat{b}_k^+ \hat{b}_k + \frac{1}{2} \right) \end{aligned} \tag{A22}$$

where k_B is Boltzmann's constant. From this we obtain

$$f_\nu(T) = \prod_k < \nu_k | \exp\left[-\frac{\hbar\omega_k}{k_B T} \left(\hat{b}_k^+ \hat{b}_k + \frac{1}{2} \right) \right] | \nu_k > \tag{A23}$$

For the moment we can drop the index k and calculate only one factor of the product:

$$< \nu | \exp\left[-\frac{\hbar\omega}{k_B T} \left(\hat{b}^+ \hat{b} + \frac{1}{2} \right) \right] | \nu > = e^{-\frac{\hbar\omega}{2k_B T}} < \nu | e^{-\frac{\hbar\omega}{k_B T} \hat{b}^+ \hat{b}} | \nu > = e^{-\frac{\hbar\omega}{2k_B T}} \sum_{\mu=0}^{\infty} \frac{\left(-\frac{\hbar\omega}{k_B T} \right)^\mu}{\mu!} < \nu | \left(\hat{b}^+ \hat{b} \right)^\mu | \nu > =$$

$$= e^{-\frac{\hbar\omega}{2k_B T}} \sum_{\mu=0}^{\infty} \frac{\left(-\frac{\hbar\omega}{k_B T} \right)^\mu}{\mu!} \nu^\mu < \nu | \nu > = \exp\left[-\frac{\hbar\omega}{k_B T} \left(\nu + \frac{1}{2} \right) \right] \tag{A24}$$

since

$$\hat{b}^+ \hat{b} | \nu > = \sqrt{\nu}\, \hat{b}^+ | \nu - 1 > = \nu | \nu > \quad \Rightarrow \quad \left(\hat{b}^+ \hat{b} \right)^\mu | \nu > = \nu^\mu | \nu > \tag{A25}$$

Therefore we obtain for the product

$$f_\nu(T)=\prod_k \exp\left[-\frac{\hbar\omega_k}{k_BT}\left(\nu_k+\frac{1}{2}\right)\right]=\left\{\prod_{k'}\exp\left[-\frac{\hbar\omega_{k'}}{2k_BT}\right]\right\}\cdot\left\{\prod_k\exp\left[-\frac{\hbar\omega_k}{k_BT}\nu_k\right]\right\} \tag{A26}$$

and thus we can cancel the factors containing the zero-point vibrations from our weight factor:

$$\rho_\nu(T)=\frac{\exp\left[-\sum_k\frac{\hbar\omega_k}{k_BT}\nu_k\right]}{\sum_{\{\nu_{k'}\}=0}^{\infty}\exp\left[-\sum_{k'}\frac{\hbar\omega_{k'}}{k_BT}\nu_{k'}\right]} \tag{A27}$$

where the summation symbol indicates that each ν_k (k = 1 to N–1, translational mode excluded) has to be summed independently from 0 to infinity.

Note that our expression for $L_\nu{}^t$ does not depend on ν, and therefore

$$L^t(T)=\sum_\nu\rho_\nu(T)L^t_\nu=L^t\sum_\nu\rho_\nu=L^t\quad\text{since}\quad\sum_\nu\rho_\nu(T)=1 \tag{A28}$$

where $L^t=L_\nu{}^t$ (A21). Thus our Lagrangian becomes

$$L(T)=L^t-H(T)\quad;\quad H(T)=\sum_\nu\rho_\nu(T)H_\nu \tag{A29}$$

and the Euler-Lagrange equations of the second kind for our unknown parameters are:

$$\frac{d}{dt}\frac{\partial L(T)}{\partial\dot{x}^*_q}-\frac{\partial L(T)}{\partial x^*_q}=0\quad;\quad\{x^*_q\}=\{a^*_n,b^*_{nk}\}\quad;\quad\Rightarrow\quad\frac{d}{dt}\frac{\partial L^t}{\partial\dot{x}^*_q}-\frac{\partial L^t}{\partial x^*_q}+\frac{\partial H(T)}{\partial x^*_q}=0 \tag{A30}$$

because $H(\underline{T})$ does not depend on the time derivatives. Note, that exactly at this point the critiques set in, because in principle one would have to compute the dynamics of the ansatz states for any set $\{\nu_k\}$, form expectation values and then perform the thermal average on these expectation values, e.g. the probability to find an amide-I quantum at site n, $P_n(\nu)$, should be computed as

$$|\varphi_\nu(t)>=|D_1(t),\nu>\quad;\quad\frac{d}{dt}\frac{\partial L_\nu}{\partial\dot{x}^*_q}-\frac{\partial L_\nu}{\partial x^*_q}=0\quad;\quad P_n(\nu)=<\varphi_\nu(t)|\hat{a}^+_n\hat{a}_n|\varphi_\nu(t)>\quad;\quad P_n(T)=\sum_n\rho_\nu(T)P_n(\nu) \tag{A31}$$

Since that procedure cannot be performed, Davydov suggested to form the thermal average already on the Lagrangian as an approximation.

The differentiations of L^t are trivial and yield the following equations of motion

$$\begin{aligned}-i\hbar\left[\dot{a}_n+\frac{1}{2}\sum_k\left(\dot{b}_{nk}b^*_{nk}-b_{nk}\dot{b}^*_{nk}\right)a_n\right]+\frac{\partial H(T)}{\partial a^*_n}&=0\\ -i\hbar\left[\dot{b}_{nk}|a_n|^2+\frac{1}{2}b_{nk}\left(\dot{a}_na^*_n+a_n\dot{a}^*_n\right)\right]+\frac{\partial H(T)}{\partial b^*_{nk}}&=0\end{aligned} \tag{A32}$$

Thus as next step we have to compute the expectation value of the Hamiltonian and subsequently its thermal average. For this purpose we calculate first the overlaps $D_{nm}(\nu)$ of two coherent states

$$D_{nm}(\nu) = <\beta_n,\nu|\beta_m,\nu> = <\nu|\hat{U}_n^+\hat{U}_m|\nu> \tag{A33}$$

With the help of Hausdorff's theorem the two coherent displacement operators can be rewritten to

$$\begin{aligned}\hat{U}_m &= e^{-\frac{1}{2}\sum_k |b_{mk}|^2} e^{\sum_k b_{mk}\hat{b}_k^+} e^{-\sum_k b_{mk}^*\hat{b}_k} \\ \hat{U}_n^+ &= e^{\frac{1}{2}\sum_k |b_{nk}|^2} e^{\sum_k b_{nk}^*\hat{b}_k} e^{-\sum_k b_{nk}\hat{b}_k^+}\end{aligned} \tag{A34}$$

which yields

$$D_{nm}(\nu) = \gamma_{nm} <\nu| e^{\sum_k b_{nk}^+\hat{b}_k} e^{\sum_k (b_{mk}-b_{nk})\hat{b}_k^+} e^{-\sum_k b_{mk}^+\hat{b}_k} |\nu> \quad ; \quad \gamma_{nm} = e^{\frac{1}{2}\sum_k \left(|b_{nk}|^2-|b_{mk}|^2\right)} \tag{A35}$$

Applying again Hausdorff's theorem in the form

$$e^{\alpha\hat{b}} e^{\beta\hat{b}^+} = e^{\alpha\beta} e^{\beta\hat{b}^+} e^{\alpha\hat{b}} \tag{A36}$$

yields

$$\begin{aligned}D_{nm}(\nu) = D_{nm}(0) B_{nm}(\nu) \quad ; \quad B_{nm}(\nu) &= <\nu| e^{\sum_k a_{nm,k}\hat{b}_k^+} e^{-\sum_k a_{nm,k}^*\hat{b}_k} |\nu> \quad ; \quad a_{nm,k} = b_{mk} - b_{nk} \\ D_{nm}(0) &= \exp\left\{\sum_k \left[b_{nk}^* b_{mk} - \frac{1}{2}\left(|b_{nk}|^2 + |b_{mk}|^2\right)\right]\right\}\end{aligned} \tag{A37}$$

The desired quantity is

$$D_{nm}(T) = D_{nm}(0) \sum_\nu \rho_\nu(T)\, B(\nu) \tag{A38}$$

The factors occurring can be rewritten to

$$\begin{aligned}B_{nm}(\nu) &= \prod_k <\nu_k| e^{a_{nm,k}\hat{b}_k^+} e^{-a_{nm,k}^*\hat{b}_k} |\nu_k> \equiv \prod_k B_{nm,k}(\nu_k) \\ \rho_\nu(T) &= \prod_k \frac{\exp[-\alpha_k\nu_k]}{\sum_{\mu_k=0}^{\infty}\exp[-\alpha_k\mu_k]} \quad ; \qquad \alpha_k = \frac{\hbar\omega_k}{k_B T} \\ D_{nm}(T) &= D_{nm}(0)\prod_k A_{nm,k}(T) \quad ; \quad A_{nm,k}(T) = \frac{\sum_{\nu_k=0}^{\infty} B_{nm,k}(\nu_k) e^{-\alpha_k\nu_k}}{\sum_{\mu_k=0}^{\infty} e^{-\alpha_k\mu_k}}\end{aligned} \tag{A39}$$

Since we are faced with a product of independent factors, we can drop the indices n, m and k from now on and compute

$$A = \frac{\sum_{\nu=0}^{\infty} B_\nu e^{-\alpha\nu}}{\sum_{\mu=0}^{\infty} e^{-\alpha\mu}} \quad ; \quad B_\nu = <\nu| e^{a\hat{b}^+} e^{-a^*\hat{b}} |\nu> \tag{A40}$$

Expansion of the exponentials yields

$$B_\nu = \sum_{\sigma,\kappa=0}^{\infty} \frac{a^\sigma \left(-a^*\right)^\kappa}{\sigma!\,\kappa!} <\nu| \left(\hat{b}^+\right)^\sigma \hat{b}^\kappa |\nu> \quad ; \quad \hat{b}^\kappa |\nu> = \sqrt{\frac{\nu!}{(\nu-\kappa)!}} |\nu-\kappa> \Theta(\kappa,\nu)$$
$$<\nu| \left(\hat{b}^+\right)^\sigma = \sqrt{\frac{\nu!}{(\nu-\sigma)!}} <\nu-\sigma| \Theta(\sigma,\nu) \quad ; \qquad \Theta(\mu,\nu) = \begin{cases} 0 & ; \quad \mu > \nu \\ 1 & ; \quad 0 \le \mu \le \nu \end{cases} \tag{A41}$$

Thus we have

$$<\nu-\sigma|\nu-\kappa> = \delta_{\sigma,\kappa} \quad \Rightarrow \quad B_\nu = \sum_{\sigma=0}^{\nu} \frac{\left(-|a|^2\right)}{(\sigma!)^2} \frac{\nu!}{(\nu-\sigma)!} = \sum_{\sigma=0}^{\nu} \Omega_{\sigma\nu} \quad ; \quad \Omega_{\sigma\nu} = \frac{\left(-|a|^2\right)^\sigma}{\sigma!} \binom{\nu}{\sigma} \tag{A42}$$

Therefore our final quantity A consists of the ratio of two infinite summations:

$$A = \frac{X}{S} \quad ; \quad X = \sum_{\nu=0}^{\infty} B_\nu e^{-\alpha\nu} \quad ; \quad S = \sum_{\nu=0}^{\infty} e^{-\alpha\nu} \quad ; \quad S = \sum_{\nu=0}^{\infty} q^\nu \quad ; \quad 0 < q = e^{-\alpha} < 1 \quad ; \quad \text{since } \alpha > 0$$
$$S = \frac{1}{1-q} = \left(1 - e^{-\alpha}\right)^{-1} \tag{A43}$$

The last equlity holds because S is a simple geometric series. Assuming X to be absolutely convergent, we can rearrange it:

$$X = \sum B_\nu e^{-\alpha\nu} = \sum\sum \Omega_{\mu\nu} e^{-\alpha\nu} = \Omega_{00} + \left(\Omega_{01} + \Omega_{11}\right) e^{-\alpha} + \left(\Omega_{02} + \Omega_{12} + \Omega_{22}\right) e^{-2\alpha} + \ldots =$$
$$= \sum_{\nu=0}^{\infty} \Omega_{0\nu} e^{-\nu\alpha} + e^{-\alpha} \sum_{\nu=1}^{\infty} \Omega_{1\nu} e^{-(\nu-1)\alpha} + e^{-2\alpha} \sum_{\nu=2}^{\infty} \Omega_{2\nu} e^{-(\nu-2)\alpha} + \ldots =$$
$$= \sum_{\mu=0}^{\infty} \Omega_{0\mu} e^{-\mu\alpha} + e^{-\alpha} \sum_{\mu=0}^{\infty} \Omega_{1,\mu+1} e^{-\mu\alpha} + e^{-2\alpha} \sum_{\mu=0}^{\infty} \Omega_{2,\mu+2} e^{-\mu\alpha} + \ldots = \sum_{\nu=0}^{\infty} e^{-\nu\alpha} \sum_{\mu=0}^{\infty} \Omega_{\nu,\mu+\nu} e^{-\mu\alpha} \tag{A44}$$

and obtain finally

$$X = \sum_{\nu=0}^{\infty} e^{-\nu\alpha} \frac{\left(-|a|^2\right)^\nu}{\nu!} \sum_{\mu=0}^{\infty} \binom{\mu+\nu}{\nu} e^{-\mu\alpha} = \sum_{\nu=0}^{\infty} \frac{x^\nu}{\nu!} \sum_{\mu=0}^{\infty} \binom{\mu+\nu}{\nu} y^\mu$$
$$x \equiv -|a|^2 e^{-\alpha} \quad ; \quad x^\nu = e^{-\nu\alpha} \left(-|a|^2\right)^\nu \quad ; \quad y \equiv e^{-\alpha} \quad ; \quad y^\mu = e^{-\mu\alpha} \tag{A45}$$

Now one can prove by complete induction that

$$\nu!\sum_{\mu=0}^{\infty}\binom{\mu+\nu}{\nu}y^{\mu}=\frac{d^{\nu}}{dy^{\nu}}\sum_{\mu=0}^{\infty}y^{\mu} \tag{A46}$$

holds. Since y is smaller than 1, the geometric series and all its derivatives with respect to y are absolutely convergent, and differentiation and summation can be interchanged, what is necessary for the steps of the prove. The geometric series can be performed and the result differentiated:

$$\sum_{\mu=0}^{\infty}\binom{\mu+\nu}{\nu}y^{\mu}=\frac{1}{\nu!}\frac{d^{\nu}}{dy^{\nu}}\sum_{\mu=0}^{\infty}y^{\mu}=\frac{1}{\nu!}\frac{d^{\nu}}{dy^{\nu}}(1-y)^{-1}$$

$$\text{because}\quad \frac{d^{\nu}}{dy^{\nu}}(1-y)^{-1}=\nu!(1-y)^{-(\nu+1)} \tag{A47}$$

with the help of this result we can reduce the second summation over ν to the Taylor series for an exponential which converges absolutely with infinite radius of convergence:

$$X=\sum_{\nu=0}^{\infty}\frac{x^{\nu}}{\nu!}(1-y)^{-(\nu+1)}=(1-y)^{-1}\sum_{\nu=0}^{\infty}\frac{1}{\nu!}\left[x(1-y)^{-1}\right]^{\nu}=S\cdot e^{\frac{x}{1-y}}$$

$$\frac{x}{1-y}=\frac{-|a|^2\,e^{-\alpha}}{1-e^{-\alpha}}=\frac{-|a|^2}{e^{\alpha}-1}\quad;\quad S=\frac{1}{1-y}\quad;\quad A=\frac{X}{S}=\exp\left[-\frac{|a|^2}{e^{\alpha}-1}\right]=e^{-|\alpha|^2\nu}\quad;\quad \nu\equiv\left(e^{\alpha}-1\right)^{-1} \tag{A48}$$

As next step we want to show what is the meaning of ν, which we simply have defined in eq. (A48). For this purpose we want to calculate the thermal average of the number of phonons in normal mode k, ν_k, using eq. (A27) in product form:

$$v_k=\sum_{\nu}\nu_k\rho_{\nu}(T)=\frac{\sum_{\nu_k=0}^{\infty}\nu_k\exp\left[-\frac{\hbar\omega_k}{k_BT}\nu_k\right]}{\sum_{\mu_k=0}^{\infty}\exp\left[-\frac{\hbar\omega_k}{k_BT}\mu_k\right]}\cdot W_k\quad;\quad W_k=\left[\prod_{k'\neq k}\frac{\sum_{\nu_k=0}^{\infty}\exp\left[-\frac{\hbar\omega_{k'}}{k_BT}\nu_{k'}\right]}{\sum_{\mu_k=0}^{\infty}\exp\left[-\frac{\hbar\omega_k}{k_BT}\mu_k\right]}\right]=1 \tag{A49}$$

Dropping again the indices for a while, we obtain

$$v=\frac{\sum_{\nu=1}^{\infty}\nu e^{-\nu\alpha}}{\sum_{\mu=0}^{\infty}e^{-\mu\alpha}}=\frac{e^{\alpha}\sum_{\nu=1}^{\infty}\nu e^{-\nu\alpha}}{e^{\alpha}\sum_{\mu=0}^{\infty}e^{-\mu\alpha}}=\frac{\sum_{\nu=1}^{\infty}\nu e^{-(\nu-1)\alpha}}{e^{\alpha}\sum_{\mu=0}^{\infty}e^{-\mu\alpha}}=\frac{\sum_{\nu=0}^{\infty}(\nu+1)e^{-\nu\alpha}}{e^{\alpha}\sum_{\mu=0}^{\infty}e^{-\mu\alpha}}=\frac{\sum_{\nu=0}^{\infty}\nu e^{-\nu\alpha}+\sum_{\nu=0}^{\infty}e^{-\nu\alpha}}{e^{\alpha}\sum_{\mu=0}^{\infty}e^{-\mu\alpha}}=e^{-\alpha}\left[\frac{\sum_{\nu=0}^{\infty}\nu e^{-\nu\alpha}}{\sum_{\mu=0}^{\infty}e^{-\mu\alpha}}+1\right]$$

$$\Rightarrow\quad v=e^{-\alpha}(v+1)\quad\Rightarrow\quad\frac{e^{-\alpha}}{1-e^{-\alpha}}=\frac{1}{e^{\alpha}-1} \tag{A50}$$

This makes clear that the quantitity ν as defined above is nothing else than the thermal average of the initial occupation numbers (incoherent) of the normal modes.

Now we can introduce the indices again:

$$A_{nm,k}(T) = e^{-|a_{nm,k}(T)|^2 \nu_k} \quad ; \quad D_{nm}(T) = D_{nm}(0) \prod_k A_{nm,k}(T) \tag{A51}$$

Thus we can write down our final results

$$D_{nm}(T) = \sum_\nu \rho_\nu(T) < \beta_n, \nu | \beta_m, \nu > = D_{nm}(0) A_{nm}(T)$$

$$D_{nm}(0) = \exp\left\{ \sum_k \left[b^*_{nk} b_{mk} - \frac{1}{2}\left(|b_{nk}|^2 + |b_{mk}|^2 \right) \right] \right\} = \exp\left[-\frac{1}{2} \sum_k \left(|b_{nk} - b_{mk}|^2 + b_{nk} b^*_{mk} - b^*_{nk} b_{mk} \right) \right]$$

$$A_{nm}(T) = \exp\left[-\sum_k \nu_k |b_{nk} - b_{mk}|^2 \right] = \exp\left\{ \sum_k \nu_k \left[b^*_{nk} b_{mk} + b_{nk} b^*_{mk} - \left(|b_{nk}|^2 + |b_{mk}|^2 \right) \right] \right\} \tag{A52}$$

$$\nu_k = \left[\exp\left(\frac{\hbar \omega_k}{k_B T} \right) - 1 \right]^{-1} \quad ; \quad \lim_{T \to 0} \nu_k = 0$$

Note, that Cruzeiro et al. [17] come to identical results in their derivations.

Now we are in the position to compute the thermally averaged Hamiltonian and its derivatives. The expectation values of the phonon operators occuring and the themal averages of all terms containing explicitely í in any form were derived above. For the operators of the amide-I oscillators we have only simple relations

$$\begin{aligned} &{}_e\!<0|\hat{a}^+_n \hat{a}_m|0>_e = 0 \; ; \quad {}_e\!<0|\hat{a}_n \hat{a}^+_m|0>_e = {}_e\!<0|\delta_{nm} + \hat{a}^+_m \hat{a}_n|0>_e = \delta_{nm} \\ &{}_e\!<0|\hat{a}_m \hat{a}^+_n \hat{a}_{n'} \hat{a}^+_{m'}|0>_e = {}_e\!<0|(\delta_{mn} + \hat{a}^+_n \hat{a}_m)(\delta_{m'n'} + \hat{a}^+_{m'} \hat{a}_{n'})|0>_e = \delta_{mn} \delta_{m'n'} \end{aligned} \tag{A53}$$

for the expectation values needed for the computation of $H_í$. The Hamiltonian is

$$\hat{H} = \varepsilon_0 \sum_n \hat{a}^+_n \hat{a}_n - J \sum_n \left(\hat{a}^+_n \hat{a}_{n+1} + \hat{a}^+_{n+1} \hat{a}_n \right) + \sum_k \hbar \omega_k \left(\hat{b}^+_k \hat{b}_k + \frac{1}{2} \right) + \sum_{nk} \hbar \omega_k B_{nk} \left(\hat{b}^+_k + \hat{b}_k \right) \hat{a}^+_n \hat{a}_n \tag{A54}$$

$$H_\nu = < D_1, \nu | \hat{H} | D_1, \nu >$$

and the expectation value consequently

$$H_\nu = \varepsilon_0 \sum_n |a_n|^2 - J \sum_n a^*_n \left[a_{n+1} D_{n,n+1}(\nu) + a_{n-1} D_{n,n-1}(\nu) \right] + \sum_{nk} \hbar \omega_k \left[B_{nk} \left(b_{nk} + b^*_{nk} \right) + |b_{nk}|^2 + \nu_k + \frac{1}{2} \right] |a_n|^2 \tag{A55}$$

The thermal averages of the ν-containing terms have been derived above and thus we obtain in agreement with [17]

$$H(T) = \sum_\nu \rho_\nu(T) H_\nu =$$

$$\varepsilon_0 \sum_n |a_n|^2 - J \sum_n a^*_n \left[a_{n+1} D_{n,n+1}(T) + a_{n-1} D_{n,n-1}(T) \right] + \sum_{nk} \hbar \omega_k \left[B_{nk} \left(b_{nk} + b^*_{nk} \right) + |b_{nk}|^2 + \nu_k + \frac{1}{2} \right] |a_n|^2 \tag{A56}$$

The differentiation of H(T) with respect to a_n^* yields inserted into the first line of eq. (A32)

$$i\hbar\,\dot{a}_n = -\frac{i\hbar}{2}\sum_k\left(\dot{b}_{nk}\,b_{nk}^* - \dot{b}_{nk}^*\,b_{nk}\right)a_n + \varepsilon_0\,a_n - J\left[\,a_{n+1}D_{n,n+1}(T) + a_{n-1}D_{n,n-1}(T)\right] + \\ + \sum_k \hbar\omega_k\left[\,B_{nk}\left(b_{nk}+b_{nk}^*\right) + |b_{nk}|^2 + v_k + \frac{1}{2}\right]a_n \tag{A57}$$

Multiplying our coefficients a_n with a phase:

$$a_n = \exp\left\{-\frac{it}{\hbar}\left[\varepsilon_0 + \sum_k \hbar\omega_k\left(v_k+\frac{1}{2}\right)\right]\right\}c_n \quad ; \quad a_n a_m^* = c_n c_m^* \tag{A58}$$

we obtain finally

$$i\hbar\,\dot{c}_n = -\frac{i\hbar}{2}\sum_k\left(\dot{b}_{nk}\,b_{nk}^* - \dot{b}_{nk}^*\,b_{nk}\right)c_n - J\left[\,c_{n+1}D_{n,n+1}(T) + c_{n-1}D_{n,n-1}(T)\right] + \sum_k \hbar\omega_k\left[\,B_{nk}\left(b_{nk}+b_{nk}^*\right) + |b_{nk}|^2\,\right]c_n \tag{A59}$$

Differentiation of $H(T)$ with respect to b_{nk}^*yields

$$i\hbar|c_n|^2\,\dot{b}_{nk} = -\frac{i\hbar}{2}\left(\dot{c}_n c_n^* + c_n\dot{c}_n^*\right)b_{nk} + \hbar\omega_k\left(B_{nk}+b_{nk}\right)|c_n|^2 - J\sum_m c_m^*\left[c_{m+1}\frac{\partial}{\partial b_{nk}^*}D_{m,m+1}(T) + c_{m-1}\frac{\partial}{\partial b_{nk}^*}D_{m,m-1}(T)\right] \tag{A60}$$

Note, that the phase factors at the a_n cancel out already in $H(T)$. From (A59) we obtain

$$\alpha_n = i\hbar\frac{d}{dt}|c_n|^2 = i\hbar\left(\dot{c}_n^* c_n + c_n\dot{c}_n^*\right) = -J\left[c_{n+1}D_{n,n+1}(T) + c_{n-1}D_{n,n-1}(T)\right]c_n^* + J\left[c_{n+1}^*D_{n+1,n}(T) + c_{n-1}^*D_{n-1,n}(T)\right]c_n \tag{A61}$$

Thus the norm N of our state is conserved

$$i\hbar\dot{N} = i\hbar\frac{d}{dt}\sum_n |a_n|^2 = i\hbar\frac{d}{dt}\sum_n |c_n|^2 = \sum_n \alpha_n = 0 \tag{A62}$$

The differentiation of the D's is trivial:

$$\frac{\partial}{\partial b_{nk}^*}D_{m,m\pm1}(T) = \left[\left(v_k+1\right)b_{n\pm1,k}\delta_{mn} + v_k b_{n\mp1,k}\delta_{m,n\mp1} - \left(v_k+\frac{1}{2}\right)b_{nk}\left(\delta_{mn}+\delta_{m,n\mp1}\right)\right]D_{m,m\pm1}(T) \tag{A63}$$

This together with the explicit form of α_n yields, after division by $|c_n|^2$, the final equations of motion for the b_{nk}:

$$i\hbar\dot{b}_{nk} = \hbar\omega_k\left(B_{nk}+b_{nk}\right) + J\left\{\left(b_{nk}-b_{n+1,k}\right)\left[\left(v_k+1\right)D_{n,n+1}(T)\frac{c_{n+1}}{c_n} + v_k D_{n+1,n}(T)\frac{c_{n+1}^*}{c_n^*}\right] + \right. \\ \left. + \left(b_{nk}-b_{n-1,k}\right)\left[\left(v_k+1\right)D_{n,n-1}(T)\frac{c_{n-1}}{c_n} + v_k D_{n-1,n}(T)\frac{c_{n-1}^*}{c_n^*}\right]\right\} \tag{A64}$$

Note finally that for T = 0 K, $v_k(T=0) = 0$, and thus the conventional $|D_1\rangle$ equations are obtained.

Appendix B: Spectrum for an Initial One-Site Excitation in a Decoupled Open Chain of Amide-I Oscillators

In a decoupled chain of amide-I oscillators we have the state

$$|\varphi(t)> = e^{-\frac{it}{\hbar}\left(\varepsilon_0+\frac{1}{2}\sum_K \hbar\Omega_K\right)}\sum_{n=1}^{N} a_n(t)\hat{a}_n^+(t)|0> \tag{B1}$$

where in the exponent we have the zero-point energy of the lattice phonons (the lattice is still present, although it is decoupled) and ε_0=0.205 eV. The $a_n(t)$ obey the equations of motion

$$\begin{aligned} &i\hbar\dot{\underline{a}} = \underline{\underline{J}}\,\underline{a} \;\; ; \;\; \underline{\underline{W}}^+\,\underline{\underline{J}}\,\underline{\underline{W}} = \underline{\underline{\varepsilon}} \;\; ; \;\; \varepsilon_{kk'} = \varepsilon_k\delta_{kk'} \;\; ; \;\; J_{n'n} = -J\left[\delta_{n',n+1}(1-\delta_{nN}) + \delta_{n',n-1}(1-\delta_{n1})\right] \\ &\varepsilon_k = -2J\cos\left[\frac{\pi}{N+1}k\right] \;\; ; \;\; W_{nk} = \sqrt{\frac{2}{N+1}}\sin\left(\frac{\pi}{N+1}nk\right) \;\; ; \;\; n,k = 1,\ldots,N\,; \;\; N \text{ arbitrary} \end{aligned} \tag{B2}$$

This is easily solved via

$$i\hbar\,\underline{\underline{W}}^+\,\underline{a} = \underline{\underline{W}}^+\,\underline{\underline{J}}\,\underline{\underline{W}}\,\underline{\underline{W}}^+\,\underline{a} \;\; \Rightarrow \;\; i\hbar\dot{\underline{c}} = \underline{\underline{\varepsilon}}\,\underline{c} \;\; ; \;\; \underline{c} = \underline{\underline{W}}^+\,\underline{a} \tag{B3}$$

The diagonal system of equations for $\underline{c}$ can be directly integrated between 0 and t (the initial excitation is at site o) and yields

$$a_n(t) = \sum_{k=1}^{N} W_{nk}W_{ok}^* e^{-\frac{it}{\hbar}\varepsilon_k} \;; \;\; a_n(0) = \delta_{on} \tag{B4}$$

Thus the time dependent state (which solves the time dependent Schrödinger equation for the decoupled system with the lattice in its equilibrium exactly, as shown in [14]) is

$$|\varphi(t)> = e^{-\frac{it}{\hbar}\left(\varepsilon_0+\frac{1}{2}\sum_K \hbar\Omega_K\right)}\sum_{n,k=1}^{N} W_{nk}W_{ok}^* e^{-\frac{it}{\hbar}\varepsilon_k}\hat{a}_n^+|0> \;\; ; \;\; |\varphi(0)> = \hat{a}_0^+|0> \tag{B5}$$

and consequently the autocorrelation function:

$$S(t) = <\varphi(0)|\varphi(t)> = e^{-\frac{it}{2\hbar}\sum_K \hbar\Omega_K}\sum_{k=1}^{N}|W_{ok}|^2 e^{-i\omega_k t} \;\; ; \;\; \omega_k = \frac{1}{\hbar}(\varepsilon_0+\varepsilon_k) \tag{B6}$$

Thus the absorption cross section is given by

$$\sigma(\omega) = 8\pi^2\alpha a_0^2\omega\,\mathrm{Re}\left[\int_0^\infty e^{\frac{it}{\hbar}\left(\hbar\omega+\frac{1}{2}\sum_K\hbar\Omega_K\right)}S(t)\,dt\right] = 4\pi^2\alpha a_0^2\omega\sum_{k=1}^{N}|W_{ok}|^2\int_{-\infty}^{\infty}e^{i(\omega-\omega_k)t}dt = 8\pi^3\alpha a_0^2\omega\sum_{k=1}^{N}|W_{ok}|^2\,\delta(\omega-\omega_k) \tag{B7}$$

From this it is obvious that in contrast to periodic boundary conditions, in the open chain now we have a weighted superposition of delta peaks, where the weight just represents the splitting as discussed in the main text for the coupled case also. Therefore this splitting cannot be viewed as a signature of soliton formation.

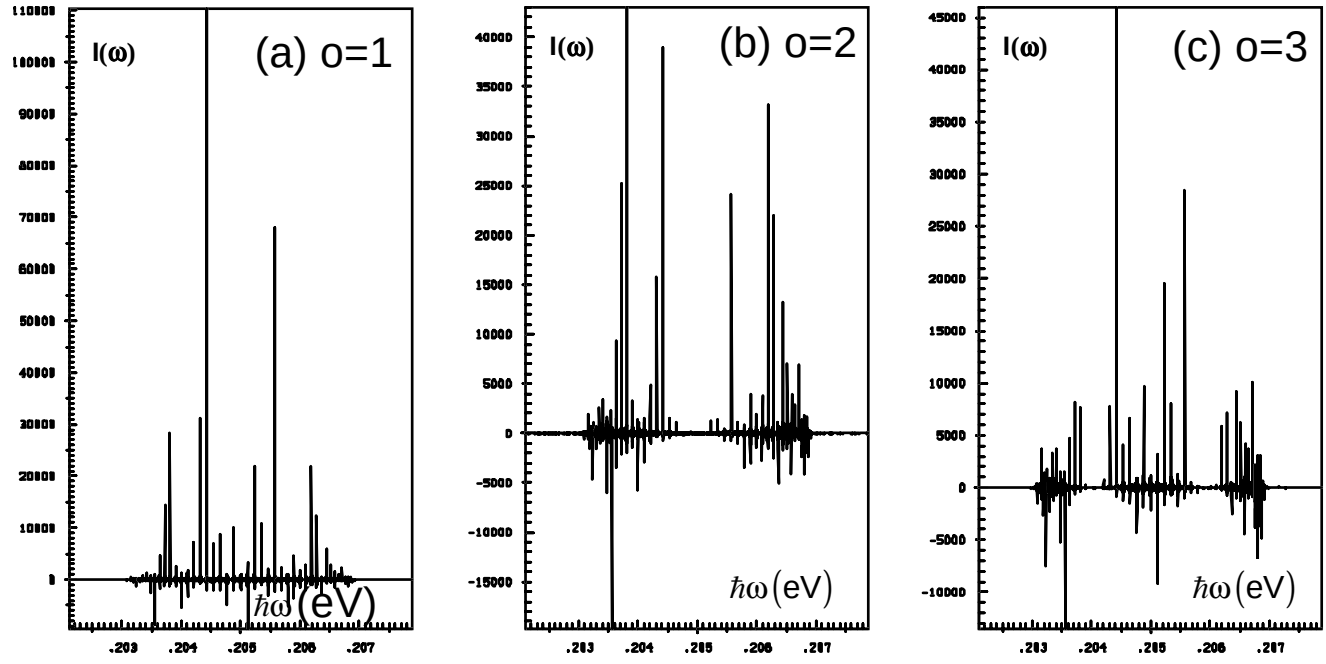

Figure 14. *Absorption cross section I (in arbitrary units) as function of the frequency ω of the incident radiation for the case of free dispersion, calculated with eq. (B8) for an open chain of 51 units, J = 0.967 meV, an initial one-site excitation at site o and T = 3 ms for*
(a) o = 1 (b) o = 2 (c) o = 3

Note finally, that for the case of a finite simulation time (T) we would obtain

$$\sigma(\omega) = 8\pi^2\alpha a_0^2\omega\sum_{k=1}^{N}|W_{ok}|^2\int\cos(\omega-\omega_k)t\,dt = 8\pi^2\alpha a_0^2\omega\sum_{k=1}^{N}|W_{ok}|^2\frac{\sin(\omega-\omega_k)T}{\omega-\omega_k}$$

$$\sigma(\omega_k) = 8\pi^2\alpha a_0^2\omega\left[|W_{ok}|^2\,T+\sum_{\substack{k'=1\\k'\neq k}}^{N}|W_{o'k}|^2\frac{\sin(\omega_k-\omega_{k'})T}{\omega_k-\omega_{k'}}\right] \qquad \text{(B8)}$$

This shows, that in case of small T it is possible to obtain artificially negative values for the cross section. Figure 14 shows spectra obtained with eq. (B8) for an example of T = 3 ms and three different initial excitation sites. Obviously, the splitting which was observed in Figure 8 occurs qualitatively also in this case of free dispersion. However, the finite time T makes the spectra less regular than those obtained in systems containing solitons.